Use of algebraic dual spaces in domain decomposition methods for Darcy flow in 3D domains

Jain, V.; Palha, A.; Gerritsma, M.

DOI
10.1016/j.cma.2022.115827

Publication date
2023

Document Version
Final published version

Published in
Computer Methods in Applied Mechanics and Engineering

Available online at www.sciencedirect.com
ScienceDirect
Comput. Methods Appl. Mech. Engrg. 404 (2023) 115827
Computer methods in applied mechanics and engineering
www.elsevier.com/locate/cma

Use of algebraic dual spaces in domain decomposition methods for Darcy flow in 3D domains

V. Jain*, A. Palha, M. Gerritsma

Delft University of Technology, Faculty of Aerospace Engineering, P.O. Box 5058, 2600 GB Delft, The Netherlands

Received 22 March 2022; received in revised form 21 November 2022; accepted 24 November 2022
Available online xxxx

Abstract

In this work we use algebraic dual spaces with a domain decomposition method to solve the Darcy equations. We define the broken Sobolev spaces and their finite dimensional counterparts. A global trace space is defined that connects the solution between the broken spaces. Use of algebraic dual spaces results in a sparse, metric-free representation of the incompressibility constraint, the pressure gradient term, and on the continuity constraint between the sub domains. To demonstrate this, we solve two test cases: (i) a manufactured solution case, and (ii) an industrial benchmark reservoir modelling problem SPE10. The results demonstrate that the dual spaces can be used for domain decomposition formulation, and despite having more unknowns, requires less simulation time compared to the continuous Galerkin formulation, without compromising on the accuracy of the solution.

Keywords: Domain decomposition; Algebraic dual spaces; Darcy equations; SPE10; Mimetic spectral element method; Hybrid finite elements

1. Introduction

Since the early days of computational fluid dynamics there has been an immense increment in computational power. However, the need to develop fast numerical algorithms has persisted consistently. For that reason, domain decomposition (DD) methods have played an important role in reducing the run times for numerical simulations. The general idea for these methods is that the domain of the problem is broken up into a set of many small independent sub domains. New degrees of freedom are introduced, the Lagrange multipliers, imposing the appropriate continuity constraints across these sub domains. It is then possible to solve for the coupled system of Lagrange multiplier equations only, which is a smaller system compared to the continuous unbroken formulation. The local solution in the sub domains is obtained independently of each other. The connection between sub domains is ensured by the Lagrange multipliers that act as local boundary conditions. This process reduces the computational burden of the problem in the sense that it is less demanding in terms of required memory and computational time, without compromising on the accuracy of the results. Over the last decades, many variants of DD methods have been developed, for example, hybrid method [1–3], Steklov–Poincaré method [4,5], FETI method [6,7], mortar method [8]. The differentiating factor between all these methods is the choice of discretization of the Lagrange

* Corresponding author.
E-mail address: V.Jain@tudelft.nl (V. Jain).

https://doi.org/10.1016/j.cma.2022.115827

multiplier space, and whether the Lagrange multipliers act as Dirichlet or Neumann boundary conditions. The hybrid methods are perhaps the earliest implementation of DD methods [9], and were developed for conforming mesh elements. The Steklov–Poincaré methods take a different approach, where they develop a Dirichlet to Neumann operator for sub domain boundaries that is used to impose the continuity across mesh elements. FETI methods were developed to deal with sub domains with non-matching grids on their interface [10], and the mortar methods can have different discretization methods on different sub domains [11]. In case of matching interface conditions, all the methods result in the same discretization. A comprehensive discussion of these methods is given in [12,13]. The two main challenges for DD methods are: (i) to find a subset of suitable finite element spaces such that the system matrices are not singular, i.e. they do not produce spurious kinematic modes [14], especially with respect to the trace spaces of the Lagrange multipliers; and (ii) how to efficiently solve the global system of Lagrange multiplier equations which can become large for practical applications and are characterized by high condition number. The primary objective of this paper addresses the first challenge where we want to show that the algebraic dual spaces introduced in [15], for 3D hexahedron elements, can be used with a DD formulation for solving Darcy flow. In this paper, we use the finite element spaces developed for the mimetic spectral element method in [15–18]. While conventional finite element formulations only use nodal degrees of freedom, mimetic methods assign the degrees of freedom to geometric objects. In this way there will be degrees of freedom associated to nodes, edges, surfaces, and volumes of the mesh. These degrees of freedom are associated to the whole geometric object and not just to a particular location in the object. The novel aspect of this paper is glueing together surface degrees of freedom between neighbouring sub domains using algebraic dual spaces. In this paper, we only use conforming mesh interfaces, and therefore we use a hybrid based DD formulation.

It is shown that the use of dual spaces results in a sparse, metric-free representation for the divergence constraint on the velocity, the pressure gradient term, and the continuity constraint across the sub domain, even for high order spectral element methods. We also see that the continuity constraints are local to the boundary face of the adjoining sub domain. In this work we use a dual space construction similar to the one in [8], but different in terms of finite element used to construct the primal spaces.

In this paper we use 3D hexahedron spectral elements of order $N = 1, 2, 3$ and demonstrate the advantage of using algebraic dual spaces with the DD formulation, using two test cases. The first test case is a manufactured solution taken from [19] on an arbitrarily deformed smooth domain. Using this case we first show that the DD formulation gives the same solution as the continuous formulation, and requires shorter simulation times. It is observed that the speed-up in simulation time is more in case of large problems. We also show optimal rates of convergence upon mesh refinement. The second test case is a benchmark reservoir modelling test case SPE10 [20] that demonstrates the use of this formulation on a practical application. The purpose of this work is threefold: (i) to demonstrate that the dual spaces can be extended to the framework of DD methods without compromising on accuracy of the results, (ii) the use of dual spaces is more efficient in a DD formulation in terms of simulation time, and (iii) to show the applicability of the method for industrial benchmark problems such as the SPE10 case.

This paper is structured as follows: In Section 2 we define the broken Sobolev spaces for the DD formulation. In Section 3 we define the finite element spaces. In Section 4 we derive the weak formulation of this problem for the DD method. The discrete formulation for this problem and the solution steps are also described in this section. In Section 5 we present the results for the two test cases, (i) the manufactured test case from [19], and (ii) the benchmark test case SPE10 [20]. We draw conclusions and discuss the scope for future work in Section 6.

2. Broken Sobolev spaces

Let $\Omega \subset \mathbb{R}^3$ be a bounded domain with Lipschitz boundary $\partial\Omega$. The equations for the Darcy problem in the domain Ω are given by

$$\begin{cases} \boldsymbol{u} + \mathbb{K}\ \text{grad}\ p & = 0 \\ \text{div}\ \boldsymbol{u} & = f \end{cases} \quad \text{with} \quad \begin{cases} \boldsymbol{u}\cdot\boldsymbol{n} = \hat{u} & \text{on} \quad \Gamma_N \\ p = \hat{p} & \text{on} \quad \Gamma_D \\ \Gamma_N \cap \Gamma_D = \emptyset & \text{and} \quad \Gamma_N \cup \Gamma_D = \partial\Omega \end{cases}, \tag{1}$$

where $\boldsymbol{u}$ is the velocity vector field, $\mathbb{K}$ is the symmetric, positive definite permeability tensor, p is the pressure, f is the given right hand side term, $\boldsymbol{n}$ is the outward unit normal vector, $\hat{u}$ is the given velocity boundary condition imposed on Neumann boundary Γ_N and $\hat{p}$ is the pressure boundary condition imposed on the Dirichlet boundary Γ_D.

Let $L^2(\Omega)$ be the space of square integrable functions and $[L^2(\Omega)]^3$ the space of square integrable vector fields in 3D, and $H^1(\Omega)$, $H(\text{div};\Omega)$ be the Hilbert spaces defined as

$$\begin{aligned} H^1(\Omega) &:= \left\{ p \in L^2(\Omega) : \text{grad } p \in [L^2(\Omega)]^3 \right\} \\ H(\text{div};\Omega) &:= \left\{ \boldsymbol{v} \in [L^2(\Omega)]^3 : \text{div } \boldsymbol{v} \in L^2(\Omega) \right\} \end{aligned} .$$

The trace spaces $H^{1/2}(\partial\Omega)$ and $H^{-1/2}(\partial\Omega)$ are dual to each other, and defined as

$$\begin{aligned} H^{1/2}(\partial\Omega) &:= \left\{ \lambda : \exists\ p \in H^1(\Omega) \quad \text{s.t.} \quad \lambda = p|_{\partial\Omega} \right\} \\ H^{-1/2}(\partial\Omega) &:= \{ \mu : \exists\ \boldsymbol{v} \in H(\text{div};\Omega) \quad \text{s.t.} \quad \boldsymbol{v}\cdot\boldsymbol{n}|_{\partial\Omega} = \mu \} \end{aligned} .$$

Let Ω be broken into T non-overlapping open sub domains $\mathcal{M}_i \subset \Omega$ with Lipschitz boundary $\partial\mathcal{M}_i$, $i = 1, \dots, T$, such that

$$\Omega = \bigcup_{i=1,\dots,T} \overline{\mathcal{M}}_i \qquad \text{and} \qquad \mathcal{M}_i \bigcap \mathcal{M}_j = \emptyset \quad \text{for} \quad i \neq j \ . \tag{2}$$

Let Ω_T be the set of sub domains, and $\partial\Omega_T$ be the set of boundaries of these sub domains defined as

$$\Omega_T = \{\mathcal{M}_i\}_{i=1,\dots,T} \qquad \partial\Omega_T = \{\partial\mathcal{M}_i\}_{i=1,\dots,T} \ .$$

We define the broken Sobolev spaces for the set of sub domains Ω_T as

$$\begin{aligned} L^2(\Omega_T) &:= \prod_{\mathcal{M}\in\Omega_T} L^2(\mathcal{M}) \ , \\ H(\text{div};\Omega_T) &:= \prod_{\mathcal{M}\in\Omega_T} H(\text{div};\mathcal{M}) \ , \\ H^{-1/2}(\partial\Omega_T) &:= \prod_{\Gamma\in\partial\Omega_T} H^{-1/2}(\Gamma) \ . \end{aligned}$$

The boundary interface between two domains $\mathcal{M}_i$ and $\mathcal{M}_j$ will be denoted by $\overset{\circ}{\Gamma}_{ij}$, such that

$$\overset{\circ}{\Gamma}_{ij} = \partial\mathcal{M}_i \bigcap \partial\mathcal{M}_j \ , \qquad \text{for} \qquad 1 \leq i < j \leq T \ ,$$

and the set of these interfaces as

$$\overset{\circ}{\Gamma} = \left\{ \overset{\circ}{\Gamma}_{ij} \right\}_{1\leq i<j\leq T} .$$

The interface between a sub domain $\mathcal{M}_i$ and boundary of the domain is denoted by

$$\Gamma_{\partial\Omega,i} = \left\{ \gamma_i = \partial\mathcal{M}_i \bigcap \partial\Omega \qquad \text{for} \qquad 1 \leq i \leq T \right\} \ .$$

and the collection of all such interfaces is given by $\Gamma_{\partial\Omega} = \left\{ \Gamma_{\partial\Omega,i} \right\}_{1\leq i\leq T}$. The combined set of internal, $\overset{\circ}{\Gamma}$, and boundary, $\Gamma_{\partial\Omega}$, interfaces is given by

$$\overline{\Gamma} = \overset{\circ}{\Gamma} \cup \Gamma_{\partial\Omega} \ .$$

We define the interface space as

$$H^{1/2}\left(\overline{\Gamma}\right) := \left\{ \lambda \ ; \exists\ p_i \in H^1(\mathcal{M}_i),\ p_j \in H^1(\mathcal{M}_j) \mid p_i|_{\partial\mathcal{M}_i\cap\partial\mathcal{M}_j} = p_j\big|_{\partial\mathcal{M}_i\cap\partial\mathcal{M}_j} = \lambda \right\} \ . \tag{3}$$

3. Finite element spaces

We will use the definition of finite element (FE) in terms of the triplet Ω, V, $\mathcal{N}$, where Ω is a compact, connected Lipschitz domain; V is a finite dimensional linear vector space of scalar or vector fields; $\mathcal{N}$ is a set of linear functionals acting on elements of V, also known as local degrees of freedom. Furthermore, there exists a basis Ψ in V, such that

$$\mathcal{N}_i^k\left(\Psi_j^k\right) = \delta_{ij} \ , \qquad 1 \leq i, j \leq d_V \ ,$$

where d_V is the dimension of the linear vector space, and k is the dimension of the geometric object (nodes, line segments, surfaces or volumes) associated with the FE, on which $\mathcal{N}_i^k$ is defined. The degrees of freedom are defined as integrals of the function over the geometric object associated with the FE, for eg. see (9) and (12).

We can represent any $p \in V$ as

$$p(\boldsymbol{x}) = \sum_{i=1}^{d_V} \mathcal{N}_i^k(p)\, \Psi_i^k(\boldsymbol{x}) \, .$$

To simplify the notation, we will write the basis functions as row vectors and degrees of freedom as column vectors

$$\Psi^k(\boldsymbol{x}) = \begin{pmatrix} \Psi_1^k(\boldsymbol{x}) & \Psi_2^k(\boldsymbol{x}) & \dots & \Psi_{d_\mathcal{V}}^k(\boldsymbol{x}) \end{pmatrix} \quad \text{and} \quad \mathcal{N}^k(p) = \begin{pmatrix} \mathcal{N}_1^k(p) \\ \mathcal{N}_2^k(p) \\ \vdots \\ \mathcal{N}_{d_\mathcal{V}-1}^k(p) \\ \mathcal{N}_{d_\mathcal{V}}^k(p) \end{pmatrix} .$$

Therefore, any element $p \in V$ can be represented as

$$p(\boldsymbol{x}) = \Psi^k(\boldsymbol{x})\, \mathcal{N}^k(p) \, . \tag{4}$$

3.1. The algebraic dual space

Definition 1. We define the dual degrees of freedom and the dual basis functions as [15]: For $\alpha \in \widetilde{V}$

$$\widetilde{\mathcal{N}}^{3-k}(\alpha) := \mathbb{M}^{(k)} \mathcal{N}^k(\alpha) \, , \tag{5}$$

$$\widetilde{\Psi}^{3-k}(\boldsymbol{x}) := \Psi^k(\boldsymbol{x}) \left(\mathbb{M}^{(k)}\right)^{-1} , \tag{6}$$

where $\mathbb{M}^{(k)}$ is the mass matrix associated with $\Psi^k(\boldsymbol{x})$ basis, $\mathbb{M}^{(k)} = \int_\Omega \Psi^k(\boldsymbol{x})^\intercal \, \Psi^k(\boldsymbol{x}) \, \mathrm{d}\Omega$.

Remark 1. The FE constructed in [15] are associated to the geometric objects of the mesh, i.e. points, line segments, surfaces, and volumes, with geometric dimensions $k = 0, 1, 2, 3$ respectively. The dimension of the geometric object, k, will be denoted as a superscript on the basis functions and degrees of freedom as Ψ^k, $\mathcal{N}^k$.

In case of dual FE, the geometric dimensions are associated to geometric dual objects, therefore dimension $(3-k)$. The basis functions and degrees of freedom are then denoted as $\widetilde{\Psi}^{3-k}$, $\widetilde{\mathcal{N}}^{3-k}$, respectively.

Corollary 1. *The duality pairing is the bilinear form between an element of a function space and an element of its dual space. Let p, q be functions expanded in terms of primal and dual FE spaces V, $\widetilde{V}$ respectively. Their duality pairing is then defined as*

$$\langle q, p \rangle := \int_\Omega q(\boldsymbol{x})\, p(\boldsymbol{x}) \, \mathrm{d}\Omega = \widetilde{\mathcal{N}}^{3-k}(q)^\intercal \left(\int_\Omega \widetilde{\Psi}^{3-k}(\boldsymbol{x})^\intercal \, \Psi^k(\boldsymbol{x}) \, \mathrm{d}\Omega \right) \mathcal{N}^k(p) = \widetilde{\mathcal{N}}^{3-k}(q)^\intercal \, \mathcal{N}^k(p) \, , \tag{7}$$

where the angled brackets denote the duality pairing. In (7), we see that the duality pairing between the elements of the primal and the dual spaces is equal to the vector dot product between the expansion coefficients of the primal and the dual space. It does not require calculation of dense mass matrices.

3.2. FE spaces for continuous Galerkin formulation

In this section we describe the construction of FE spaces for spectral element methods developed in [16–18], and the algebraic dual spaces developed in [15].

Consider the 1D domain $\widehat{\Omega} = [-1, 1]$. Let ξ_i, for $i = 0, \dots, N$ be the Gauss–Lobatto–Legendre nodes of polynomial degree N defined on $\widehat{\Omega}$. Let h_i, for $i = 0, \dots, N$ be the set of Lagrange polynomials through the GLL

nodes. We define the edge polynomials e_i, for $i = 1, \ldots, N$ of polynomial degree $N-1$ as

$$e_i \coloneqq -\sum_{j=0}^{i-1} \frac{\mathrm{d}h_j}{\mathrm{d}\xi} \, . \tag{8}$$

The basis e_i satisfies the Kronecker-delta property in an integral sense, i.e.

$$\int_{\xi_{j-1}}^{\xi_j} e_i \, \mathrm{d}\xi = \delta_{ij} \, .$$

In the following section we will use the tensor product of 1D Lagrange polynomials, h_i, and the edge polynomials, e_j to form FE spaces for a 3D hexahedron.

Now, consider the reference domain $\widehat{\Omega} = [-1, 1]^3$. Let ξ_i, η_j, ζ_k, $i, j, k = 0, \ldots, N$, be the GLL nodes in the ξ, η, ζ- directions. Let $s_i^{\xi}, s_j^{\eta}, s_k^{\zeta}$, $i, j, k = 1, \ldots, N^2(N+1)$ be the surfaces of the GLL mesh with unit normal in ξ, η, ζ direction, respectively. Let v_i, $i = 1, \ldots, N^3$ be the volumes of the GLL mesh.

For an arbitrary domain $\Omega \subset \mathbb{R}^3$ let Φ be the diffeomorphism between the reference domain $\widehat{\Omega} = [-1, 1]^3$ and Ω, such that $\Omega = \Phi\left(\widehat{\Omega}\right)$. For any scalar function $\widehat{p} \in V\left(\widehat{\Omega}\right)$, $p \in V(\Omega)$ is given by $p(\boldsymbol{x}) = \widehat{p} \circ \Phi^{-1}(\boldsymbol{x})$. In Cartesian coordinates, we introduce the Jacobian tensor J as

$$J \coloneqq \begin{bmatrix} \frac{\partial \Phi^x}{\partial \xi} & \frac{\partial \Phi^x}{\partial \eta} & \frac{\partial \Phi^x}{\partial \zeta} \\ \frac{\partial \Phi^y}{\partial \xi} & \frac{\partial \Phi^y}{\partial \eta} & \frac{\partial \Phi^y}{\partial \zeta} \\ \frac{\partial \Phi^z}{\partial \xi} & \frac{\partial \Phi^z}{\partial \eta} & \frac{\partial \Phi^z}{\partial \zeta} \end{bmatrix},$$

where, Φ^x, Φ^y, Φ^z- are x, y, z components of the map Φ.

3.2.1. Finite element space $D(\Omega) \subset H(\mathrm{div}; \Omega)$

For any vector field $\boldsymbol{q} \in D(\widehat{\Omega})$ we introduce the local degrees of freedom as integral over the surfaces of the GLL mesh as

$$\begin{cases} \mathcal{N}_i^{2,\xi}(\boldsymbol{q}) & \coloneqq \int_{s_i^{\xi}} \left(\boldsymbol{q}(\xi_i, \eta, \zeta) \cdot \boldsymbol{e}_{\xi}\right) \mathrm{d}\eta \, \mathrm{d}\zeta \quad i = 1, \ldots, N^2(N+1) \\ \mathcal{N}_j^{2,\eta}(\boldsymbol{q}) & \coloneqq \int_{s_j^{\eta}} \left(\boldsymbol{q}\left(\xi, \eta_j, \zeta\right) \cdot \boldsymbol{e}_{\eta}\right) \mathrm{d}\xi \, \mathrm{d}\zeta \quad j = 1, \ldots, N^2(N+1) \\ \mathcal{N}_k^{2,\zeta}(\boldsymbol{q}) & \coloneqq \int_{s_k^{\zeta}} \left(\boldsymbol{q}(\xi, \eta, \zeta_k) \cdot \boldsymbol{e}_{\zeta}\right) \mathrm{d}\xi \, \mathrm{d}\eta \quad k = 1, \ldots, N^2(N+1) \end{cases},$$

where we use $'2'$ in the superscript to denote that degrees of freedom are sampled over surfaces. It can be shown that the basis function that satisfy the Kronecker-delta property are given by

$$\begin{cases} \widehat{\Psi}_{i,j,k}^{2,\xi}(\xi, \eta, \zeta) & \coloneqq h_i(\xi) e_j(\eta) e_k(\zeta) \boldsymbol{e}_{\xi} \quad i = 0, \ldots, N; \, j, k = 1, \ldots, N \\ \widehat{\Psi}_{i,j,k}^{2,\eta}(\xi, \eta, \zeta) & \coloneqq e_i(\xi) h_j(\eta) e_k(\zeta) \boldsymbol{e}_{\eta} \quad i, k = 1, \ldots, N; \, j = 0, \ldots, N \\ \widehat{\Psi}_{i,j,k}^{2,\zeta}(\xi, \eta, \zeta) & \coloneqq e_i(\xi) e_j(\eta) h_k(\zeta) \boldsymbol{e}_{\zeta} \quad i, j = 1, \ldots, N; k = 0, \ldots, N \end{cases}.$$

For ease of notation, we collect the basis functions in the matrix as

$$\begin{aligned} \widehat{\Psi}^2(\boldsymbol{\xi}) &\coloneqq \begin{bmatrix} \widehat{\Psi}_1^{2,\xi}(\boldsymbol{\xi}) & \ldots & \widehat{\Psi}_{N(N+1)^2}^{2,\xi}(\boldsymbol{\xi}) & & & & & & \\ & & & \widehat{\Psi}_1^{2,\eta}(\boldsymbol{\xi}) & \ldots & \widehat{\Psi}_{N(N+1)^2}^{2,\eta}(\boldsymbol{\xi}) & & & \\ & & & & & & \widehat{\Psi}_1^{2,\zeta}(\boldsymbol{\xi}) & \ldots & \widehat{\Psi}_{N(N+1)^2}^{2,\zeta}(\boldsymbol{\xi}) \end{bmatrix} \\ &= \begin{bmatrix} \widehat{\Psi}_{\xi}^2(\boldsymbol{\xi}) & 0 & 0 \\ 0 & \widehat{\Psi}_{\eta}^2(\boldsymbol{\xi}) & 0 \\ 0 & 0 & \widehat{\Psi}_{\zeta}^2(\boldsymbol{\xi}) \end{bmatrix}. \end{aligned}$$

In case of an arbitrary domain $\Omega \subset \mathbb{R}^3$, the local degrees of freedom are introduced as

$$\mathcal{N}^2(\boldsymbol{q}) = \begin{cases} \mathcal{N}_i^{2,\xi}(\boldsymbol{q}) & \coloneqq \int_{\Phi\left(s_i^{\xi}\right)} \boldsymbol{q}(\boldsymbol{x}) \cdot \boldsymbol{e}_{\xi} \mathrm{d}S \quad i = 1, \ldots, N^2(N+1) \\ \mathcal{N}_j^{2,\eta}(\boldsymbol{q}) & \coloneqq \int_{\Phi\left(s_j^{\eta}\right)} \boldsymbol{q}(\boldsymbol{x}) \cdot \boldsymbol{e}_{\eta} \mathrm{d}S \quad j = 1, \ldots, N^2(N+1) \\ \mathcal{N}_k^{2,\zeta}(\boldsymbol{q}) & \coloneqq \int_{\Phi\left(s_k^{\zeta}\right)} \boldsymbol{q}(\boldsymbol{x}) \cdot \boldsymbol{e}_{\zeta} \mathrm{d}S \quad k = 1, \ldots, N^2(N+1) \end{cases}, \tag{9}$$

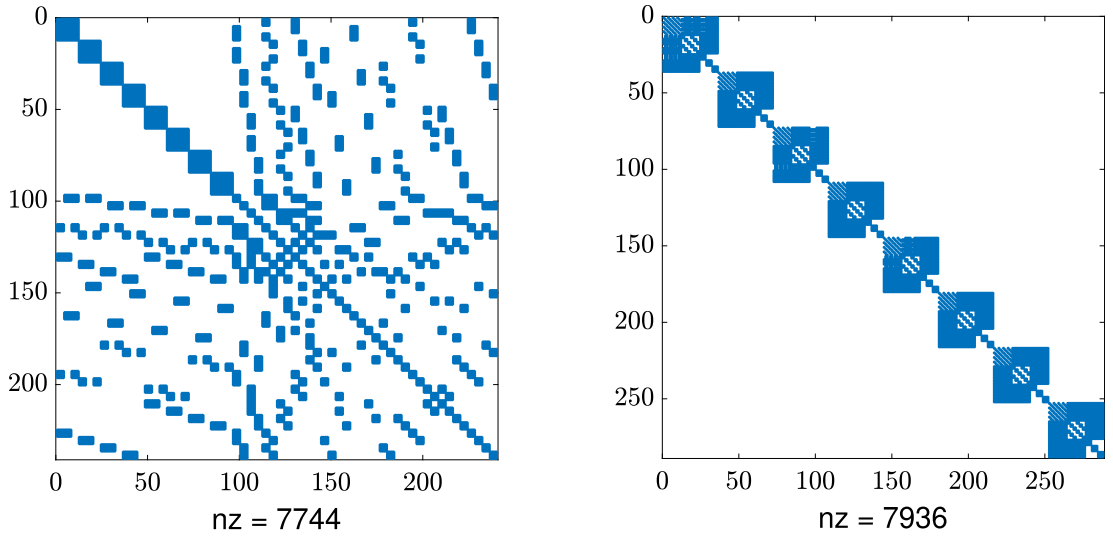

Fig. 1. Sparsity plots for the global mass matrix, for total number of elements, $K = 2 \times 2 \times 2$, $N = 2$: (i) Left: For the continuous Galerkin formulation, (ii) Right: For the DD formulation..

and the basis functions that satisfy the Kronecker-delta property are given by

$$\Psi^2(\boldsymbol{x}) = \frac{J^{-1} \circ \Phi^{-1}(\boldsymbol{x})}{\det J(\boldsymbol{x})} \widehat{\Psi}^2 \circ \Phi^{-1}(\boldsymbol{x}) \ .$$

For two elements $\boldsymbol{p}, \boldsymbol{q} \in D(\Omega)$ the L^2-inner product is given by

$$(\boldsymbol{p}, \boldsymbol{q}) = \int_\Omega \boldsymbol{p}(\boldsymbol{x}) \boldsymbol{q}(\boldsymbol{x}) \, \mathrm{d}\Omega = \mathcal{N}^2(\boldsymbol{p})^\intercal \left(\int_\Omega \Psi^2(\boldsymbol{x})^\intercal \Psi^2(\boldsymbol{x}) \, \mathrm{d}\Omega \right) \mathcal{N}^2(\boldsymbol{q}) = \mathcal{N}^2(\boldsymbol{p})^\intercal \mathbb{M}^{(2)} \mathcal{N}^2(\boldsymbol{q}) \ ,$$

where $\mathbb{M}^{(2)}$ is the mass matrix associated with the $D(\Omega)$ basis functions.

In case of a given symmetric positive definite anisotropic tensor $\mathbb{K}$, the weighted inner product is given by

$$\begin{aligned} \left(\boldsymbol{p}, \mathbb{K}^{-1}\boldsymbol{q}\right) &= \int_\Omega \boldsymbol{p}(\boldsymbol{x}) \, \mathbb{K}^{-1}(\boldsymbol{x}) \boldsymbol{q}(\boldsymbol{x}) \, \mathrm{d}\Omega \\ &= \mathcal{N}^2(\boldsymbol{p})^\intercal \left(\int_\Omega \Psi^2(\boldsymbol{x})^\intercal \, \mathbb{K}^{-1}(\boldsymbol{x}) \, \Psi^2(\boldsymbol{x}) \, \mathrm{d}\Omega \right) \mathcal{N}^2(\boldsymbol{q}) \\ &= \mathcal{N}^2(\boldsymbol{p})^\intercal \, \mathbb{M}^{(2)}_{\mathbb{K}^{-1}} \mathcal{N}^2(\boldsymbol{q}) \ . \end{aligned} \tag{10}$$

In case of multiple elements, the global degrees of freedom and the basis functions are obtained by standard FE assembly over all the elements. The vector fields in $D(\Omega) \subset H(\mathrm{div}; \Omega)$ have a continuous normal component and discontinuous tangential components between the neighbouring elements. The degrees of freedom are defined at faces and therefore some elements share the same boundary face. The global matrix is NOT a block diagonal matrix.

In Fig. 1 on the left plot we show the sparsity plot for the mass matrix using continuous formulation, for the domain shown in the left plot of Fig. 2, with number of elements $= 2 \times 2 \times 2$ and polynomial order $N = 2$. This matrix is a global (non block-diagonal) matrix, and evaluating the inverse of this matrix is computationally expensive.

In the right plot, we show the sparsity structure of global weighted mass matrix of a DD formulation (discussed in Section 3.3, see (23)) with the same topological discretization. We see that in this case the mass matrix is block diagonal. The inverse of each of these blocks can be evaluated separately, i.e. independently, of each other, reducing the computational cost.

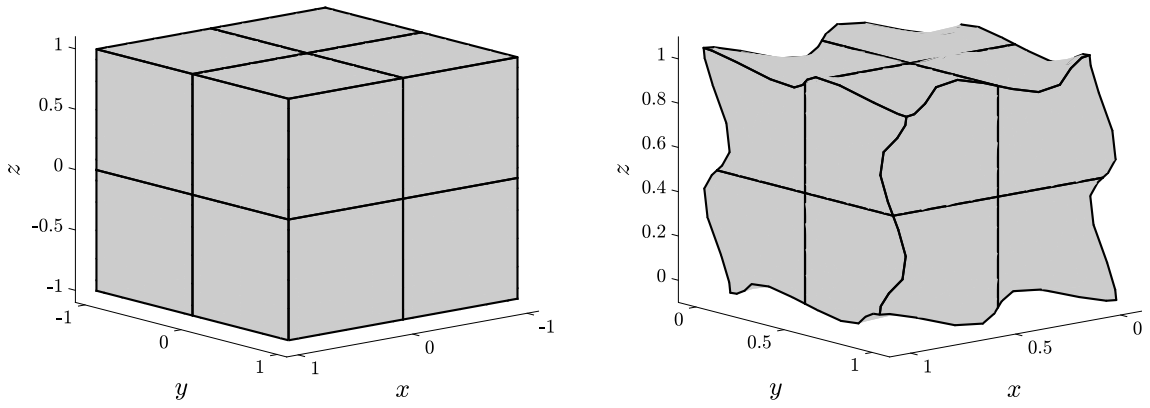

Fig. 2. Test domain with total number of elements = 3 × 3 × 3. Left: reference domain, $\widehat{\Omega}$, Right: domain of the test case, Ω.

3.2.2. The dual space $\widetilde{D}(\Omega)$

The definition for the dual space $\widetilde{D}(\Omega)$, for both single and multiple element case, follow Definition 1, i.e. the global dual degrees of freedom are obtained by pre multiplying the global primal degrees of freedom by the global mass matrix and the global dual basis functions are obtained by post multiplying the global primal basis by the inverse of the global mass matrix.

Definition 2. The degrees of freedom and basis functions for $\boldsymbol{p} \in \widetilde{D}(\Omega)$ are given by

$$\widetilde{\mathcal{N}}^1(\boldsymbol{p}) \coloneqq \mathbb{M}^{(2)}\mathcal{N}^2(\boldsymbol{p})$$
$$\widetilde{\Psi}^1(\boldsymbol{x}) \coloneqq \Psi^2(\boldsymbol{x})\left(\mathbb{M}^{(2)}\right)^{-1} .$$

The primal degrees of freedom of $D(\Omega)$ are sampled in surfaces, i.e. geometric dimension = 2. In 3D, the geometric dual of surfaces are edges, i.e. geometric dimension = 1. Therefore, following Remark 1 functions of the dual space $\widetilde{D}(\Omega)$ are represented with superscript 1 as $\widetilde{\mathcal{N}}^1$, $\widetilde{\Psi}^1$.

In practice we do not explicitly construct the dual basis functions, but only make use of the property of the dual variables given by Corollary 1.

3.2.3. The finite element space $S(\Omega) \subset L^2(\Omega)$

For any polynomial $f \in S(\widehat{\Omega})$ we introduce the local degrees of freedom as integrals evaluated over the volumes formed by the GLL mesh given by

$$\mathcal{N}^3_{(i-1)N^2+(j-1)N+k}(f) \coloneqq \int_{\xi_{i-1}}^{\xi_i}\int_{\eta_{j-1}}^{\eta_j}\int_{\zeta_{k-1}}^{\zeta_k} f(\xi,\eta,\zeta)\,\mathrm{d}\xi\,\mathrm{d}\eta\,\mathrm{d}\zeta \qquad \text{for} \qquad i,j,k = 1,\dots,N\,, \tag{11}$$

where we use the superscript $'3'$ to denote that the degrees of freedom are sampled over a volume. The basis functions that satisfy the Kronecker-delta property are given by

$$\widehat{\Psi}^3(\xi,\eta,\zeta) = \left(\ \widehat{\Psi}^3_1(\xi,\eta,\zeta) \quad \widehat{\Psi}^3_2(\xi,\eta,\zeta)\dots\widehat{\Psi}^3_{N^3}(\xi,\eta,\zeta)\ \right),$$

where,

$$\widehat{\Psi}^3_{(i-1)N^2+(j-1)N+k}(\xi,\eta,\zeta) \coloneqq e_i(\xi)\,e_j(\eta)\,e_k(\zeta) \qquad i,j,k = 1,\dots,N\,.$$

In case of an arbitrary domain $\Omega \subset \mathbb{R}^3$, we introduce the degrees of freedom as integral of the function over the mapped GLL volume given by

$$\mathcal{N}^3_{(i-1)N^2+(j-1)N+k}(f) \coloneqq \int_{\Phi\left(v_{(i-1)N^2+(j-1)N+k}\right)} f(\boldsymbol{x})\,\mathrm{d}\Omega \qquad \text{for} \qquad i,j,k = 1,\dots,N\,, \tag{12}$$

and the basis functions that satisfy the Kronecker-delta property are given by

$$\Psi^3(\boldsymbol{x}) = \frac{1}{\det J(\boldsymbol{x})} \widehat{\Psi}^3 \circ \Phi^{-1}(\boldsymbol{x}) \ .$$

For two elements $f, g \in S(\Omega)$, the L^2-inner product is given by

$$(f,g) = \int_\Omega f(\boldsymbol{x})\, g(\boldsymbol{x})\, \mathrm{d}\Omega = \mathcal{N}^3(f)^\intercal \left(\int_\Omega \Psi^3(\boldsymbol{x})^\intercal \, \Psi^3(\boldsymbol{x})\, \mathrm{d}\Omega \right) \mathcal{N}^3(g) = \mathcal{N}^3(f)^\intercal \, \mathbb{M}^{(3)} \mathcal{N}^3(g) \ , \tag{13}$$

where $\mathbb{M}^{(3)}$ is the mass matrix associated with the $S(\Omega)$ basis functions.

In case of multiple elements, the global degrees of freedom and the basis functions are obtained by standard FE assembly over all the elements.

3.2.4. The dual space $\widetilde{S}(\Omega)$

For both single and multiple element case, the definition of the dual space $\widetilde{S}(\Omega)$ follows Definition 1, i.e. the global dual degrees of freedom are obtained by pre multiplying the global primal degrees of freedom by the global mass matrix and the global dual basis functions are obtained by post multiplying the global primal basis by the inverse of the global mass matrix.

Definition 3. The local degrees of freedom and the basis functions for $f \in \widetilde{S}(\Omega)$ are given by,

$$\widetilde{\mathcal{N}}^0(f) \coloneqq \mathbb{M}^{(3)} \mathcal{N}^3(f) \tag{14}$$

$$\widetilde{\Psi}^0(\boldsymbol{x}) \coloneqq \Psi^3(\boldsymbol{x}) \left(\mathbb{M}^{(3)} \right)^{-1} \ . \tag{15}$$

Here the degrees of freedom of the primal space $S(\Omega)$ are sampled over volumes, i.e. geometric dimension $= 3$, and in 3D geometric dual of volumes is nodes with geometric dimension $= 0$. Therefore, following Remark 1, the functions of the dual space $\widetilde{S}(\Omega)$ are denoted with a superscript '0'.

Once again these operations are not performed, only the properties of dual elements are used. When we need to post process the dual variables to present its solution, we can do this on each sub-domain independently.

3.2.5. The trace space $D_b(\partial\Omega) \subset H^{-1/2}(\partial\Omega)$

Let the restriction of vector fields in $D(\Omega)$ to the domain boundary $\partial\Omega$ be denoted by $D_b(\partial\Omega)$. Let $\mathbb{N}_2$ be the inclusion matrix that maps boundary degrees of freedom to the global degrees of freedom. It is a sparse matrix which only contains the non-zero values -1 and 1. The subscript $'2'$ indicates that it maps boundary degrees of freedom associated to the surfaces with geometric dimension 2, to the global degrees of freedom.

The restriction of $\boldsymbol{q} \in D(\Omega)$ to the boundary $\partial\Omega$, is given by

$$(\boldsymbol{q} \cdot \boldsymbol{n})(\boldsymbol{x}) = \Psi^2(\boldsymbol{x}) \mathbb{N}_2 \mathbb{N}_2^\intercal \mathcal{N}^2(\boldsymbol{q}) \ , \qquad \text{for } \boldsymbol{x} \in \partial\Omega \ . \tag{16}$$

See Appendix, Example 1 on how to construct $\mathbb{N}_2$. The basis functions $\Psi_b^2(\boldsymbol{x}) = \Psi^2(\boldsymbol{x}) \mathbb{N}_2$ form a basis for the trace space $D_b(\partial\Omega)$ and the degrees of freedom $\mathcal{B}^2(\boldsymbol{q}) = \mathbb{N}_2^\intercal \mathcal{N}^2(\boldsymbol{q})$ the associated degrees of freedom. The mass matrix of this trace space is given by

$$\mathbb{M}_b^{(2)} = \int_{\partial\Omega} \Psi_b^2(\boldsymbol{x})^\intercal \, \Psi_b^2(\boldsymbol{x})\ \mathrm{d}\Gamma = \mathbb{N}_2^\intercal \mathbb{M}^{(2)} \mathbb{N}_2 \ . \tag{17}$$

3.2.6. The dual trace space $\widetilde{D}_b(\partial\Omega) \subset H^{1/2}(\partial\Omega)$

Definition 4. Using Definition 1, the degrees of freedom and the basis functions for $\hat{\phi} \in \widetilde{D}_b(\partial\Omega)$ are defied as

$$\widetilde{\mathcal{B}}^0\left(\hat{\phi}\right) = \mathbb{M}_b^{(2)} \mathcal{B}^2\left(\hat{\phi}\right) = \int_{\partial\Omega} \Psi_b^2(\boldsymbol{x})\, \hat{\phi}(\boldsymbol{x})\, \mathrm{d}\Gamma$$

$$\widetilde{\Psi}_b^0(\boldsymbol{x}) = \Psi_b^2(\boldsymbol{x}) \mathbb{M}_b^{(2)^{-1}} \ .$$

3.2.7. The divergence operator, $\mathbb{E}^{3,2}$

The divergence operator on vector functions from the space $D(\Omega)$ is defined as: $\operatorname{div} : D(\Omega) \mapsto S(\Omega)$. For any function $\boldsymbol{u} \in D(\Omega)$, we have

$$\operatorname{div} \boldsymbol{u} = \Psi^3 \mathbb{E}^{3,2} \mathcal{N}^2(\boldsymbol{u}) \ , \tag{18}$$

where $\mathbb{E}^{3,2}$ is the discrete representation of the divergence operator acting on the degrees of freedom. For the construction of $\mathbb{E}^{3,2}$, see Example 2 in Appendix. The divergence operator changes the degrees of freedom and the basis functions to that of $S(\Omega)$. The divergence operator changes the surface degrees of freedom, geometric dimension = 2, to volume degrees of freedom, geometric dimension = 3, and is therefore denoted with superscript (3, 2). The incidence matrix $\mathbb{E}^{3,2}$ is a sparse, metric free, topological and does not depend on the shape and size of the domain. For an arbitrarily shaped element the degrees of freedom and the basis functions will transform, but the incidence matrix remains the same, as long as the topology of the connections between the surfaces and the volumes remain the same.

3.2.8. The weak gradient acting on functions in dual space $\widetilde{S}(\Omega) \times \widetilde{D}_b(\partial\Omega)$

The elements of $\widetilde{S}(\Omega)$ lack regularity across the elements. Therefore, we define the weak gradient operation as

Definition 5. We define weak gradient operation as $\widetilde{\operatorname{grad}} : \widetilde{S}(\Omega) \times \widetilde{D}_b(\partial\Omega) \mapsto \widetilde{D}(\Omega)$, such that, for $(s, \hat{s}) \in \widetilde{S}(\Omega) \times \widetilde{D}_b(\partial\Omega)$

$$\int_\Omega \widetilde{\operatorname{grad}}(s, \hat{s})\, \boldsymbol{q}\, \mathrm{d}\Omega := -\int_\Omega s\, (\operatorname{div}\boldsymbol{q})\, \mathrm{d}\Omega + \int_{\partial\Omega} \hat{s}\, (\boldsymbol{q} \cdot \boldsymbol{n})\, \mathrm{d}\Gamma \qquad \forall\, \boldsymbol{q} \in D(\Omega) \ . \tag{19}$$

Since the gradient maps into $\widetilde{D}(\Omega)$, the left hand side is a duality pairing in $\widetilde{D}(\Omega) \times D(\Omega)$. The first term on the right hand side is a duality pairing in $\widetilde{S}(\Omega) \times S(\Omega)$, and the boundary integral term is the duality pairing in $\widetilde{D}_b(\partial\Omega) \times D_b(\partial\Omega)$. Therefore, using Corollary 1, we can write (19) as

$$\mathcal{N}^2(\boldsymbol{q})^\intercal \widetilde{\mathcal{N}}^1\left(\widetilde{\operatorname{grad}}(s, \hat{s})\right) = -\mathcal{N}^2(\boldsymbol{q})^\intercal \mathbb{E}^{3,2\intercal} \widetilde{\mathcal{N}}^0(s) + \mathcal{N}^2(\boldsymbol{q})^\intercal \mathbb{N}_2 \widetilde{\mathcal{B}}^0(\hat{s}) \qquad \forall\, \mathcal{N}^2(\boldsymbol{q}) \in D(\Omega) \ .$$

As the above equation needs to hold for all $\boldsymbol{q} \in D(\Omega)$, we have

$$\widetilde{\mathcal{N}}^1\left(\widetilde{\operatorname{grad}}(s, \hat{s})\right) = -\mathbb{E}^{3,2\intercal} \widetilde{\mathcal{N}}^0(s) + \mathbb{N}_2 \widetilde{\mathcal{B}}^0(\hat{s}) \ , \tag{20}$$

so the weak gradient can also be represented as a topological operation on the dual degrees of freedom, i.e. without mass matrices and only with sparse, metric-free operators and their operation on degrees of freedom. The gradient of a function in dual space is then expressed as,

$$\widetilde{\operatorname{grad}}(s, \hat{s}) = \widetilde{\Psi}^1(\boldsymbol{x}) \left(-\mathbb{E}^{3,2\intercal} \widetilde{\mathcal{N}}^0(s) + \mathbb{N}_2 \widetilde{\mathcal{B}}^0(\hat{s})\right) \ .$$

3.3. Broken finite element spaces

In this section we use finite element spaces introduced in Section 3.2 to define broken FE spaces.

3.3.1. Finite element space $D(\Omega_T) \subset H(\operatorname{div}; \Omega_T)$

For the set of domains Ω_T we define the finite element space $D(\Omega_T) \subset H(\operatorname{div}; \Omega_T)$ as

$$D(\Omega_T) := \prod_{\mathcal{M} \in \Omega_T} D(\mathcal{M}) \ . \tag{21}$$

For any two functions $\boldsymbol{u}, \boldsymbol{v} \in D(\Omega_T)$, and symmetric, positive definite permeability tensor $\mathbb{K}$, the weighted L^2-inner product is given by

$$(\boldsymbol{u}, \boldsymbol{v})_{\mathbb{K}^{-1}} = \int_\Omega \boldsymbol{u}^\intercal \mathbb{K}^{-1} \boldsymbol{v}\, \mathrm{d}\Omega = \sum_{i=1}^{T} \int_{\mathcal{M}_i} \boldsymbol{u}^\intercal \mathbb{K}^{-1} \boldsymbol{v}\, \mathrm{d}\mathcal{M} = \sum_{i=1}^{T} \mathcal{N}_i^2(\boldsymbol{u})^\intercal \mathbb{M}^{(2)}_{\mathbb{K}_i^{-1}} \mathcal{N}_i^2(\boldsymbol{v}) = \mathcal{N}^2(\boldsymbol{u})^\intercal \mathbb{M}^{(2)}_{\mathbb{K}^{-1}, hyb} \mathcal{N}^2(\boldsymbol{v}) \, , \tag{22}$$

where, $\mathcal{N}^2(\boldsymbol{u})$ and $\mathcal{N}^2(\boldsymbol{v})$ are the column vectors of assembled expansion coefficients of all the sub domains, and the mass matrix $\mathbb{M}^{(2)}_{\mathbb{K}^{-1}_{hyb}}$ is given as

$$\mathbb{M}^{(2)}_{\mathbb{K}^{-1},hyb} = \begin{bmatrix} \mathbb{M}^{(2)}_{\mathbb{K}^{-1},1} & & & \\ & \mathbb{M}^{(2)}_{\mathbb{K}^{-1},2} & & \\ & & \ddots & \\ & & & \mathbb{M}^{(2)}_{\mathbb{K}^{-1},T} \end{bmatrix}, \quad \text{with,} \qquad \mathbb{M}^{(2)}_{\mathbb{K}^{-1},i} = \int_{\mathcal{M}_i} \Psi^2_i(\boldsymbol{x})^{\intercal} \mathbb{K}^{-1}(\boldsymbol{x}) \Psi^2_i(\boldsymbol{x}) \, \mathrm{d}\mathcal{M} \,, \tag{23}$$

where $\Psi^2_i(\boldsymbol{x})$ are the basis functions associated to the finite element space $D(\mathcal{M}_i)$.

The sparsity plot of the mass matrix is shown in the right plot of Fig. 1. The inverse of this matrix can be evaluated efficiently by evaluating the inverse of the individual blocks.

3.3.2. Finite element space $S(\Omega_T) \subset L^2(\Omega_T)$

For the set of domains Ω_T we define the finite element space $S(\Omega_T) \subset L^2(\Omega_T) = L^2(\Omega)$ as

$$S(\Omega_T) \coloneqq \prod_{\mathcal{M} \in \Omega_T} S(\mathcal{M}) \,. \tag{24}$$

For elements $p, q \in S(\Omega_T)$, the L^2- inner product is given by

$$(p, q) = \int_{\Omega} p^{\intercal} q \, \mathrm{d}\Omega = \sum_{i=1}^{T} \int_{\mathcal{M}_i} p^{\intercal} q \, \mathrm{d}\mathcal{M} = \sum_{i=1}^{T} \mathcal{N}^3_i(p)^{\intercal} \mathbb{M}^{(3)}_i \mathcal{N}^3_i(q) = \mathcal{N}^3(p)^{\intercal} \mathbb{M}^{(3)}_{hyb} \mathcal{N}^3(q) \,, \tag{25}$$

where $\mathcal{N}^3(p)$, $\mathcal{N}^3(q)$ are the column vectors of assembled expansion coefficients of all the sub domains, and the mass matrix $\mathbb{M}^{(3)}_{hyb}$ is the block diagonal mass matrix given by

$$\mathbb{M}^{(3)}_{hyb} = \begin{bmatrix} \mathbb{M}^{(3)}_1 & & & \\ & \mathbb{M}^{(3)}_2 & & \\ & & \ddots & \\ & & & \mathbb{M}^{(3)}_T \end{bmatrix}, \qquad \text{with,} \qquad \mathbb{M}^{(3)}_i = \int_{\mathcal{M}_i} \Psi^3_i(\boldsymbol{x})^{\intercal} \Psi^3_i(\boldsymbol{x}) \, \mathrm{d}\mathcal{M} \,, \tag{26}$$

where $\Psi^3_i(\boldsymbol{x})$ are the basis associated with the finite element space $S(\mathcal{M}_i)$.

3.3.3. Finite dimensional space $D_b(\partial\Omega_T) \subset H^{-1/2}(\partial\Omega_T)$

For the set of boundaries $\partial\Omega_T$ we define the trace space $D_b(\partial\Omega_T) \subset H^{-1/2}(\partial\Omega_T)$ as

$$D_b(\partial\Omega_T) \coloneqq \prod_{\mathcal{M} \in \Omega_T} D_b(\partial\mathcal{M}) \,. \tag{27}$$

3.3.4. Finite dimensional space $\widetilde{S}(\Omega_T) \subset L^2(\Omega_T)$

The algebraic dual space of $S(\Omega_T)$ is denoted by $\widetilde{S}(\Omega_T)$ and defined as

$$\widetilde{S}(\Omega_T) \coloneqq \prod_{\mathcal{M} \in \Omega_T} \widetilde{S}(\mathcal{M}) \,. \tag{28}$$

Let $p, q \in S(\Omega_T) \times \widetilde{S}(\Omega_T)$, then the duality pairing between the functions is given by

$$\langle q, p \rangle = \sum_{i=1}^{T} \int_{\mathcal{M}_i} q^{\intercal} p \, \mathrm{d}\mathcal{M} = \sum_{i=1}^{T} \widetilde{\mathcal{N}}^0_i(q)^{\intercal} \mathcal{N}^3_i(p) = \widetilde{\mathcal{N}}^0(q)^{\intercal} \mathcal{N}^3(p) \,, \tag{29}$$

where, $\widetilde{\mathcal{N}}^0(q)$, $\mathcal{N}^3(p)$ are the column vectors of assembled expansion coefficients.

3.3.5. Finite dimensional space $\widetilde{D}_b\left(\overline{\Gamma}\right) \subset H^{1/2}\left(\overline{\Gamma}\right)$

Let $D_b(\gamma)$ be the space of restriction of basis of $D(\Omega_T)$ to γ, for $\gamma \in \overline{\Gamma}$, and $\widetilde{D}_b(\gamma)$, be its algebraic dual space.

Then the finite element space $\widetilde{D}_b\left(\overline{\Gamma}\right) \subset H^{1/2}\left(\overline{\Gamma}\right)$ is defined as

$$\widetilde{D}_b\left(\overline{\Gamma}\right) = \prod_{\gamma \in \overline{\Gamma}} \widetilde{D}_b(\gamma) \ . \tag{30}$$

Let $\boldsymbol{u} \in D(\Omega_T)$ be a vector field, and $\boldsymbol{u} \cdot \boldsymbol{n} \in D_b(\partial\Omega_T)$ its restriction on the sub domain boundaries. For functions $(\lambda, \boldsymbol{u} \cdot \boldsymbol{n}) \in \widetilde{D}_b\left(\overline{\Gamma}\right) \times D_b(\partial\Omega_T)$, the duality pairing is given by

$$\langle \lambda, \boldsymbol{u} \cdot \boldsymbol{n} \rangle = \sum_{i=1}^{T} \int_{\partial\mathcal{M}_i} \lambda^{\intercal}(\boldsymbol{u} \cdot \boldsymbol{n}) \, \mathrm{d}\Gamma = \sum_{i=1}^{T} \widetilde{\mathcal{B}}_i^0(\lambda)^{\intercal} \mathbb{N}_{2_i}^{\intercal} \mathcal{N}_i^2(\boldsymbol{u}) = \widetilde{\mathcal{B}}^0(\lambda)^{\intercal} \mathbb{N}_2^{\intercal} \mathcal{N}^2(\boldsymbol{u}) \ , \tag{31}$$

where $\widetilde{\mathcal{B}}^0(\lambda)$, $\mathcal{N}^2(\boldsymbol{u})$ are the column vector of assembled expansion coefficients over all sub domains and $\mathbb{N}_2^{\intercal}$ is the assembly of the inclusion matrix over all the interface and sub domain boundaries. Note that $\mathbb{N}_2$ is not block diagonal.

In this paper, we have used the same topological sub domain discretization, and therefore $\mathbb{N}_{2i}$ is the same for all the sub domains and has to be constructed only once, even if the sub domains are arbitrarily deformed.

3.3.6. The divergence operator for broken finite element spaces

Let $q, \boldsymbol{u} \in \widetilde{S}(\Omega_T) \times D(\Omega_T)$ be the elements of the broken finite dimensional spaces. Then the divergence operation on the vector field $\boldsymbol{u}$ is defined as, $\mathrm{div} : D(\Omega_T) \longrightarrow S(\Omega_T)$, such that

$$\langle q \ , \mathrm{div} \ \boldsymbol{u} \rangle \coloneqq \sum_{i=1}^{T} \int_{\mathcal{M}_i} q \ \mathrm{div} \ \boldsymbol{u} \ \mathrm{d}\mathcal{M} = \sum_{i=1}^{T} \widetilde{\mathcal{N}}_i^0(q)^{\intercal} \mathbb{E}_i^{3,2} \mathcal{N}_i^2(\boldsymbol{u}) = \widetilde{\mathcal{N}}^0(q)^{\intercal} \mathbb{E}_{hyb}^{3,2} \mathcal{N}^2(\boldsymbol{u}) \qquad \forall q \in \widetilde{S}(\Omega_T) \ , \tag{32}$$

where, $\widetilde{\mathcal{N}}^0(q), \mathcal{N}^2(\boldsymbol{u})$ are the column vectors of the assembled expansion coefficients, and $\mathbb{E}_{hyb}^{3,2}$ is the assembled divergence operator. If $\mathbb{E}_i^{3,2}$ is the discrete representation of divergence operator on the domain $\mathcal{M}_i$, then we have

$$\mathbb{E}_{hyb}^{3,2} = \begin{bmatrix} \mathbb{E}_1^{3,2} & & & \\ & \mathbb{E}_2^{3,2} & & \\ & & \ddots & \\ & & & \mathbb{E}_T^{3,2} \end{bmatrix} . \tag{33}$$

If the topology of sub domain discretizations is also the same, see Example 2, then we have that $\mathbb{E}_1^{3,2} = \mathbb{E}_2^{3,2} = \ldots = \mathbb{E}_T^{3,2}$. In this paper we have only used the case with the same topology for all the sub domains, therefore

$$\mathbb{E}_{hyb}^{3,2} = \begin{bmatrix} \mathbb{E}_o^{3,2} & & & \\ & \mathbb{E}_o^{3,2} & & \\ & & \ddots & \\ & & & \mathbb{E}_o^{3,2} \end{bmatrix} , \tag{34}$$

where $\mathbb{E}_o^{3,2}$ is the topological divergence operator for any of the sub domains.

Here note that $\mathbb{E}_o^{3,2}$ is constructed only once and used for all the sub domains, even if the sub domains are differently deformed.

3.3.7. The gradient of functions in $\widetilde{S}(\Omega_T) \times \widetilde{D}_b\left(\overline{\Gamma}\right)$

Let a scalar field, p, and its boundary values, $\hat{p}$ be expressed in terms of dual spaces. The gradient operation is then defined as: For functions $(p \ , \hat{p}) \in \widetilde{S}(\Omega_T) \times \widetilde{D}_b\left(\overline{\Gamma}\right)$, $\widetilde{\mathrm{grad}} : \widetilde{S}(\Omega_T) \times \widetilde{D}_b\left(\overline{\Gamma}\right) \to \widetilde{D}(\Omega_T)$, such that

$$\int_{\Omega} \widetilde{\mathrm{grad}}\left(p \ , \hat{p}\right) \boldsymbol{u} \ \mathrm{d}\Omega \coloneqq \sum_{i=1}^{T} \int_{\mathcal{M}_i} \widetilde{\mathrm{grad}}\left(p \ , \hat{p}\right) \boldsymbol{u} \ \mathrm{d}\mathcal{M}$$

$$= \sum_{i=1}^{T} \left(- \int_{\mathcal{M}_i} p \, (\operatorname{div} \boldsymbol{u}) + \int_{\partial \mathcal{M}_i} \hat{p} \, (\boldsymbol{u} \cdot \boldsymbol{n}) \, \mathrm{d}\Gamma \right) \quad \forall \boldsymbol{u} \in D \, (\Omega_T) \ . \tag{35}$$

In (32) the divergence operator is block diagonal, as can be seen in (33). However, the gradient operator in (35) is not block diagonal because $\hat{p} \in \widetilde{D}_b \left(\overline{\Gamma} \right)$ has global support and couples the gradients on all the sub domains together.

For the pair of $\left(p \ , \hat{p} \right) \in \widetilde{S} \, (\Omega_T) \times \widetilde{D}_b \left(\overline{\Gamma} \right)$ the weak H^1-norm is defined as

$$\| p \|^2_{H^1(\Omega)} \coloneqq \| p \|^2_{L^2(\Omega)} + \| \widetilde{\operatorname{grad}} \left(p, \, \hat{p} \right) \|^2_{L^2(\Omega)} = \sum_{i=1}^{T} \left\{ \| p \|^2_{L^2(\mathcal{M}_i)} + \| \widetilde{\operatorname{grad}} \left(p, \, \hat{p} \right) \|^2_{L^2(\mathcal{M}_i)} \right\} \ . \tag{36}$$

4. The Darcy equations

In this section we will use the broken FE spaces defined in Section 3.3 to derive the algebraic formulation for the DD formulation of the Darcy problem.

Before proceeding further we will first use the FE spaces defined in Section 3.2 to derive the continuous Galerkin formulation of Darcy problem, for comparison.

4.1. Continuous formulation

The Lagrange functional for the continuous formulation of Darcy equations is given by: For given $f \in L^2 \, (\Omega)$, $\hat{p} \in H^{1/2} \, (\Gamma_D)$, $\hat{u} \in H^{-1/2} \, (\Gamma_N)$, and the unknowns $\boldsymbol{u} \in H \, (\operatorname{div}; \, \Omega)$, $p \in L^2 \, (\Omega)$

$$\mathcal{L} \left(\boldsymbol{u}, \, p; \, f, \, \hat{p}, \, \hat{u} \right) = \int_{\Omega} \frac{1}{2} \boldsymbol{u}^{\intercal} \mathbb{K}^{-1} \boldsymbol{u} \ \mathrm{d}\Omega - \int_{\Omega} p \, (\operatorname{div} \boldsymbol{u} - f) \, \mathrm{d}\Omega + \int_{\Gamma_D} \hat{p} \, (\boldsymbol{u} \cdot \boldsymbol{n}) \, \mathrm{d}\Gamma \ , \tag{37}$$

where on the right hand side, the first term is the kinetic energy term, the second term is the constraint on divergence of velocity, and the last term weakly imposes the Dirichlet boundary conditions. The Neumann boundary conditions are implemented strongly in the trial space.

The discrete variational formulation for the above functional is given by [15, §5.2]: For given $f \in L^2 \, (\Omega)$, $\hat{p} \in H^{1/2} \, (\Gamma_D)$, find $\boldsymbol{u} \in D \, (\Omega)$, $p \in \widetilde{S} \, (\Omega)$, such that

$$\begin{cases} \left(\boldsymbol{v}, \, \mathbb{K}^{-1} \boldsymbol{u} \right) & - \langle \operatorname{div} \boldsymbol{v}, \, p \rangle & = - \left\langle \boldsymbol{v} \cdot \boldsymbol{n}, \, \hat{p} \right\rangle & \forall \boldsymbol{v} \in \ D \, (\Omega) \\ - \langle q, \operatorname{div} \boldsymbol{u} \rangle & & = - \left(q, \, f \right) & \forall q \ \in \widetilde{S} \, (\Omega) \end{cases} \ . \tag{38}$$

Using algebraic dual spaces (defined in Section 3.2) the discrete formulation is given by

$$\begin{bmatrix} \mathbb{M}^{(2)}_{\mathbb{K}^{-1}} & - \mathbb{E}^{3,2 \intercal} \\ - \mathbb{E}^{3,2} & 0 \end{bmatrix} \begin{bmatrix} \mathcal{N}^2 \, (\boldsymbol{u}) \\ \widetilde{\mathcal{N}}^0 \, (p) \end{bmatrix} = \begin{bmatrix} - \mathbb{N}_2 \widetilde{\mathcal{B}}^0 \left(\hat{p} \right) \\ - \mathcal{N}^3 \, (f) \end{bmatrix} \ , \tag{39}$$

where the inner products and duality pairing are evaluated using FE spaces for continuous Galerkin formulation as described in Section 3.2. The mass matrix $\mathbb{M}^{(2)}_{\mathbb{K}^{-1}}$ is from (10) and the incidence matrix $\mathbb{E}^{3,2}$ is from (18).

The system (39) is solved by Uzawa algorithm, where we first solve for the unknowns $\widetilde{\mathcal{N}}^0 \, (p)$ and then for the unknowns $\mathcal{N}^2 \, (\boldsymbol{u})$ as

$$\left(\mathbb{E}^{3,2} {\mathbb{M}^{(2)}_{\mathbb{K}^{-1}}}^{-1} \mathbb{E}^{3,2 \intercal} \right) \widetilde{\mathcal{N}}^0 \, (p) = \left(\mathcal{N}^3 \, (f) + \mathbb{E}^{3,2} {\mathbb{M}^{(2)}_{\mathbb{K}^{-1}}}^{-1} \mathbb{N}_2 \widetilde{\mathcal{B}}^0 \left(\hat{p} \right) \right) \ , \tag{40}$$

$$\mathbb{M}^{(2)}_{\mathbb{K}^{-1}} \mathcal{N}^2 \, (\boldsymbol{u}) = \left(\mathbb{E}^{3,2 \intercal} \widetilde{\mathcal{N}}^0 \, (p) - \mathbb{N}_2 \widetilde{\mathcal{B}}^0 \left(\hat{p} \right) \right) \ . \tag{41}$$

The left hand side matrices in the above equations are symmetric, positive definite and are therefore solved using Cholesky algorithm. Further details of computational implementation are given in Section 4.1.1.

In this formulation, no domain decomposition is applied and we will refer to this formulation from now on as the *continuous formulation*.

4.1.1. Computational implementation

The equations, (40) and (41), are solve by the Uzawa algorithm, i.e. first for degrees of freedom $\widetilde{\mathcal{N}}^0 \, (p)$, and then for degrees of freedom $\mathcal{N}^2 \, (\boldsymbol{u})$, using the Cholesky algorithm. The first step is to construct all the global matrices

Algorithm 1: Algorithm for solving the continuous formulation (39)

for *all elements* **do**
  construct $\mathbb{M}^{(2)}_{\mathbb{K}^{-1},i}$
end
construct $\mathbb{E}^{3,2}_i$
construct global $\mathbb{M}^{(2)}_{\mathbb{K}^{-1}}$ from assembly of $\mathbb{M}^{(2)}_{\mathbb{K}^{-1},i}$
construct global $\mathbb{E}^{3,2}$ from assembly of $\mathbb{E}^{3,2}_i$
evaluate and save decomposition of global $\mathbb{M}^{(2)}_{\mathbb{K}^{-1}}$
solve $\mathbb{M}^{(2)}_{\mathbb{K}^{-1}}{}^{-1}\mathbb{E}^{3,2\intercal}$ using MATLAB Cholesky solver
evaluate $\mathbb{E}^{3,2}\left(\mathbb{M}^{(2)}_{\mathbb{K}^{-1}}{}^{-1}\mathbb{E}^{3,2\intercal}\right)$
evaluate and save decomposition of $\left(\mathbb{E}^{3,2}\mathbb{M}^{(2)}_{\mathbb{K}^{-1}}{}^{-1}\mathbb{E}^{3,2\intercal}\right)$
solve (40) using MATLAB Cholesky solver
solve (41) using MATLAB Cholesky solver

on the left hand side and the right hand side of (39). In the next step, we evaluate the Cholesky decomposition of the global matrix $\mathbb{M}^{(2)}_{\mathbb{K}^{-1}}$ using MATLAB decomposition function [21]. It creates a reusable matrix decomposition, that is used again to solve (41). Then we solve $\mathbb{M}^{(2)}_{\mathbb{K}^{-1}}{}^{-1}\mathbb{E}^{3,2\intercal}$ from using the saved decomposition. Next, we evaluate $\mathbb{E}^{3,2}\left(\mathbb{M}^{(2)}_{\mathbb{K}^{-1}}{}^{-1}\mathbb{E}^{3,2\intercal}\right)$ by matrix multiplication of the global incidence matrix $\mathbb{E}^{3,2}$ with the result of the last step. Lastly, we evaluate the Cholesky decomposition of the matrix $\left(\mathbb{E}^{3,2}\mathbb{M}^{(2)}_{\mathbb{K}^{-1}}{}^{-1}\mathbb{E}^{3,2\intercal}\right)$ using the MATLAB decomposition function. We use this decomposed matrix to solve (40), for unknowns $\widetilde{\mathcal{N}}^0(p)$. Lastly, we use the decomposed matrix of $\mathbb{M}^{(2)}_{\mathbb{K}^{-1}}$ and the value of $\widetilde{\mathcal{N}}^0(p)$ evaluated in the previous step to solve (41).

4.2. The DD formulation

For the DD formulation of (1) we break the domain Ω into T sub domains, see (2), and we use the Lagrange multipliers λ to enforce the required continuity across the sub domains. The weak formulation for (1) is then obtained using the Lagrange functional given by: For given $f \in L^2(\Omega)$, $\hat{p} \in H^{1/2}(\Gamma_D)$, $\hat{u} \in H^{-1/2}(\Gamma_N)$ and the unknowns $\boldsymbol{u} \in H(\mathrm{div};\Omega_T)$, $p \in L^2(\Omega_T)$, $\lambda \in H^{1/2}\left(\overset{\circ}{\Gamma} \cup \Gamma_N\right)$

$$\mathcal{L}\left(\boldsymbol{u}, p, \lambda; f, \hat{p}, \hat{u}\right) = \sum_{i=1}^{T}\left\{\int_{\mathcal{M}_i}\frac{1}{2}\boldsymbol{u}^{\intercal}\mathbb{K}^{-1}\boldsymbol{u}\,\mathrm{d}\Omega - \int_{\mathcal{M}_i} p\,(\mathrm{div}\,\boldsymbol{u} - f)\,\mathrm{d}\Omega + \int_{\partial\mathcal{M}_i\setminus(\Gamma_D\cup\Gamma_N)}\lambda\,(\boldsymbol{u}\cdot\boldsymbol{n})\,\mathrm{d}\Gamma + \int_{\partial\mathcal{M}_i\cap\Gamma_N}\lambda\left(\boldsymbol{u}\cdot\boldsymbol{n} - \hat{u}\right)\mathrm{d}\Gamma + \int_{\partial\mathcal{M}_i\cap\Gamma_D}\hat{p}\,(\boldsymbol{u}\cdot\boldsymbol{n})\,\mathrm{d}\Gamma\right\}, \tag{42}$$

where, on the right hand side, the first term is the kinetic energy term, the second term imposes the constraint on divergence of velocity field $\boldsymbol{u}$, the third term imposes continuity of flux across the sub domain faces, the fourth term imposes the Neumann boundary condition and the fifth term imposes the Dirichlet boundary conditions.

Note that, in the third term, upon assembly over an interface Γ_{ij}, we get

$$\int_{\gamma_{ij}}\lambda\left(\boldsymbol{u}\cdot\boldsymbol{n}_i + \boldsymbol{u}\cdot\boldsymbol{n}_j\right)d\gamma = 0\,, \qquad \text{for} \qquad 1 \le i < j \le T\,,$$

where the orientation of the unit outward normals have to be taken into account. Also see Example 1, in Appendix.

The optimality conditions at the continuous level for the Lagrange functional (42) are given by: For given $f \in L^2(\Omega)$, $\hat{p} \in H^{1/2}(\Gamma_D)$, $\hat{u} \in H^{-1/2}(\Gamma_N)$, find $\boldsymbol{u} \in H(\mathrm{div};\Omega_T)$, $p \in L^2(\Omega_T)$, $\lambda \in H^{1/2}\left(\overset{\circ}{\Gamma} \cup \Gamma_N\right)$, such

that

$$\begin{cases} \left(\boldsymbol{v}, \mathbb{K}^{-1}\boldsymbol{u}\right) & -\left(\operatorname{div}\boldsymbol{v}, p\right) & +\left(\boldsymbol{v}\cdot\boldsymbol{n}, \lambda\right) & = -\left(\boldsymbol{v}\cdot\boldsymbol{n}, \hat{p}\right) & \forall \boldsymbol{v} \in H\left(\operatorname{div}; \Omega_T\right) \\ -\left(q, \operatorname{div}\boldsymbol{u}\right) & & & = -\left(q, f\right) & \forall q \in L^2\left(\Omega_T\right) \\ \left(\mu, \boldsymbol{u}\cdot\boldsymbol{n}\right) & & & = \left(\mu, \hat{u}\right) & \forall \mu \in H^{1/2}\left(\overset{\circ}{\Gamma} \cup \Gamma_N\right) \end{cases} . \tag{43}$$

The finite dimensional problem, using broken FE spaces from Section 3.3, is then given by: For given $f \in L^2\left(\Omega\right)$, $\hat{p} \in H^{1/2}\left(\Gamma_D\right)$, $\hat{u} \in H^{-1/2}\left(\Gamma_N\right)$, find $\boldsymbol{u} \in D\left(\Omega_T\right)$, $p \in \widetilde{S}\left(\Omega_T\right)$, $\lambda \in \widetilde{D}_b\left(\overset{\circ}{\Gamma} \cup \Gamma_N\right)$, such that

$$\begin{cases} \left(\boldsymbol{v}, \mathbb{K}^{-1}\boldsymbol{u}\right) & -\left\langle\operatorname{div}\boldsymbol{v}, p\right\rangle & +\left\langle\boldsymbol{v}\cdot\boldsymbol{n}, \lambda\right\rangle & = -\left(\boldsymbol{v}\cdot\boldsymbol{n}, \hat{p}\right) & \forall \boldsymbol{v} \in D\left(\Omega_T\right) \\ -\left\langle q, \operatorname{div}\boldsymbol{u}\right\rangle & & & = -\left\langle q, f\right\rangle & \forall q \in \widetilde{S}\left(\Omega_T\right) \\ \left\langle\mu, \boldsymbol{u}\cdot\boldsymbol{n}\right\rangle & & & = \left\langle\mu, \hat{u}\right\rangle & \forall \mu \in \widetilde{D}_b\left(\overset{\circ}{\Gamma} \cup \Gamma_N\right) \end{cases} . \tag{44}$$

In (44) we see that all the terms except the weighted inner product term, $\left(\boldsymbol{v}, \mathbb{K}^{-1}\boldsymbol{u}\right)$, are the duality pairing between the functions of the primal and the dual space, where we can use Corollary 1. Consequently, these terms do not require evaluation of (dense) mass matrices. The only matrices associated with these terms are the sparse, metric-free divergence operator $\mathbb{E}^{3,2}_{hyb}$, or the inclusion matrix $\mathbb{N}_2$ with non-zero entries -1 and $+1$, that have to be evaluated only once and remain the same for each sub domain. See also (45).

4.3. The algebraic formulation

The bilinear forms for the left hand side terms of (44) are evaluated as

$$\begin{aligned} &\left(\boldsymbol{v}, \mathbb{K}^{-1}\boldsymbol{u}\right) \overset{(22)}{=} \mathcal{N}^2\left(\boldsymbol{v}\right)^{\mathsf{T}} \mathbb{M}^{(2)}_{\mathbb{K}^{-1},hyb} \mathcal{N}^2\left(\boldsymbol{u}\right) , \\ &\left\langle q\ , \operatorname{div}\boldsymbol{u}\right\rangle \overset{(32)}{=} \widetilde{\mathcal{N}}^0\left(q\right)^{\mathsf{T}} \mathbb{E}^{3,2}_{hyb} \mathcal{N}^2\left(\boldsymbol{u}\right) , \\ &\left\langle\mu\ , \boldsymbol{u}\cdot\boldsymbol{n}\right\rangle \overset{(31)}{=} \widetilde{\mathcal{B}}^0\left(\mu\right)^{\mathsf{T}} \mathbb{N}_2^{\mathsf{T}} \mathcal{N}^2\left(\boldsymbol{u}\right) , \end{aligned}$$

and the projection of right hand side terms of (44) on finite element spaces are evaluated as

$$\begin{aligned} &\left\langle\boldsymbol{v}\cdot\boldsymbol{n}\ , \hat{p}\right\rangle = \sum_{i=1}^{T} \mathcal{N}^2_i\left(\boldsymbol{v}\right)^{\mathsf{T}} \mathbb{N}_{2i} \int_{\Gamma_D \cap \partial\mathcal{M}_i} \widetilde{\Psi}_{b_i}\left(\boldsymbol{x}\right) \hat{p}\left(\boldsymbol{x}\right) \mathrm{d}\Gamma = \mathcal{N}^2\left(\boldsymbol{v}\right)^{\mathsf{T}} \mathbb{N}_2 \widetilde{\mathcal{B}}^0\left(\hat{p}\right) , \\ &\left\langle q\ , f\right\rangle = \sum_{i=1}^{T} \widetilde{\mathcal{N}}^0_i\left(q\right)^{\mathsf{T}} \int_{\Omega} \widetilde{\Psi}^0_i\left(\boldsymbol{x}\right) f\left(x\right) \mathrm{d}\Omega = \widetilde{\mathcal{N}}^0\left(q\right)^{\mathsf{T}} \mathcal{N}^3\left(f\right) , \\ &\left\langle\mu\ , \hat{u}\right\rangle = \sum_{i=1}^{T} \widetilde{\mathcal{B}}^0_i\left(\mu\right)^{\mathsf{T}} \int_{\Gamma_N \cap \partial\mathcal{M}_i} \Psi^2_{b_i}\left(\boldsymbol{x}\right) \hat{u}\left(\boldsymbol{x}\right) \mathrm{d}\Gamma = \widetilde{\mathcal{B}}^0\left(\mu\right)^{\mathsf{T}} \mathbb{N}_2^{\mathsf{T}} \mathbb{N}_2 \mathcal{B}^2\left(\hat{u}\right) . \end{aligned}$$

Using the above relations we can write the discrete formulation for (44) as

$$\begin{bmatrix} \mathbb{M}^{(2)}_{\mathbb{K}^{-1},hyb} & -\mathbb{E}^{3,2\ \mathsf{T}}_{hyb} & \mathbb{N}_2 \\ -\mathbb{E}^{3,2}_{hyb} & 0 & 0 \\ \mathbb{N}_2^{\mathsf{T}} & 0 & 0 \end{bmatrix} \begin{bmatrix} \mathcal{N}^2\left(\boldsymbol{u}\right) \\ \widetilde{\mathcal{N}}^0\left(p\right) \\ \widetilde{\mathcal{B}}^0\left(\lambda\right) \end{bmatrix} = \begin{bmatrix} -\mathbb{N}_2 \widetilde{\mathcal{B}}^0\left(\hat{p}\right) \\ -\mathcal{N}^3\left(f\right) \\ \mathbb{N}_2^{\mathsf{T}} \mathbb{N}_2 \mathcal{B}^2\left(\hat{u}\right) \end{bmatrix} . \tag{45}$$

In (45), we see that the matrices $\mathbb{E}^{3,2}_{hyb}$, $\mathbb{N}_2$, are sparse and metric-free, i.e. only consist of the non-zero entries -1 and 1. By metric-free, we mean independent of the size of the elements, the shape of the elements (orthogonal or highly curved) or the order of the approximation. All the metric dependence is contained in the basis functions and therefore in the mass matrix $\mathbb{M}^{(2)}_{\mathbb{K}^{-1},hyb}$. Using static condensation (45) can be solved efficiently for the trace variables $\widetilde{\mathcal{B}}^0\left(\lambda\right)$ only. We first solve for a global system of $\widetilde{\mathcal{B}}^0\left(\lambda\right)$ by

$$\left(\mathbb{N}_2^{\mathsf{T}} \mathbb{A}_{hyb} \mathbb{N}_2\right) \widetilde{\mathcal{B}}^0\left(\lambda\right) = -\mathcal{B}^2\left(\hat{u}\right) + \mathbb{N}_2^{\mathsf{T}} \left(\mathbb{M}^{(2)}_{\mathbb{K}^{-1},hyb}{}^{-1} \mathbb{E}^{3,2\mathsf{T}}_{hyb} \left(\mathbb{E}^{3,2}_{hyb} \mathbb{M}^{(2)}_{\mathbb{K}^{-1},hyb}{}^{-1} \mathbb{E}^{3,2\ \mathsf{T}}_{hyb} \right)^{-1} \mathcal{N}^3\left(f\right) - \mathbb{A}_{hyb} \mathbb{N}_2 \widetilde{\mathcal{B}}^0\left(\hat{p}\right) \right) \tag{46}$$

where,

$$\mathbb{A}_{hyb} = {\mathbb{M}^{(2)}_{\mathbb{K}^{-1},hyb}}^{-1} - {\mathbb{M}^{(2)}_{\mathbb{K}^{-1},hyb}}^{-1} \mathbb{E}^{3,2\,\intercal}_{hyb} \left(\mathbb{E}^{3,2}_{hyb} {\mathbb{M}^{(2)}_{\mathbb{K}^{-1},hyb}}^{-1} \mathbb{E}^{3,2\,\intercal}_{hyb} \right)^{-1} \mathbb{E}^{3,2}_{hyb} {\mathbb{M}^{(2)}_{\mathbb{K}^{-1},hyb}}^{-1} .$$

The left hand side of (46) can be constructed efficiently by evaluating for each sub domain separately, as

$$\mathbb{N}^{\intercal}_{2,i} \mathbb{A}_i \mathbb{N}_{2,i} = \mathbb{N}^{\intercal}_{2,i} {\mathbb{M}^{(2)}_{\mathbb{K}^{-1},i}}^{-1} \mathbb{N}_{2,i} - \mathbb{N}^{\intercal}_{2,i} {\mathbb{M}^{(2)}_{\mathbb{K}^{-1},i}}^{-1} \mathbb{E}^{3,2\,\intercal}_{i} \left(\mathbb{E}^{3,2}_{i} {\mathbb{M}^{(2)}_{\mathbb{K}^{-1},i}}^{-1} \mathbb{E}^{3,2\intercal}_{i} \right)^{-1} \mathbb{E}^{3,2}_{i} {\mathbb{M}^{(2)}_{\mathbb{K}^{-1},i}}^{-1} \mathbb{N}_{2,i} , \tag{47}$$

and then assembling over all the sub domains. The matrices $\mathbb{M}^{(2)}_{\mathbb{K}^{-1},i}$ and $\left(\mathbb{E}^{3,2}_{i} {\mathbb{M}^{(2)}_{\mathbb{K}^{-1},i}}^{-1} \mathbb{E}^{3,2\intercal}_{i} \right)$ in (47) are symmetric, positive definite. We use the Cholesky decomposition of these matrices to evaluate (47). The left hand side of (46) is also symmetric, positive definite and the λ is solved using Cholesky algorithm. Once the interface variables λ are solved, the local degrees of freedom in sub domains $\mathcal{M}_i$, $i = 1, \ldots, T$ are then evaluated, as

$$\left(\mathbb{E}^{3,2}_{i} {\mathbb{M}^{(2)}_{\mathbb{K}^{-1},i}}^{-1} \mathbb{E}^{3,2\intercal}_{i} \right) \widetilde{\mathcal{N}}^0_i (p) = \left(\mathcal{N}^3_i (f) + \mathbb{E}^{3,2}_{i} {\mathbb{M}^{(2)}_{\mathbb{K}^{-1},i}}^{-1} \mathbb{N}_{2i} \left(\widetilde{\mathcal{B}}^0_i \left(\hat{p} \right) + \widetilde{\mathcal{B}}^0_i (\lambda) \right) \right) \tag{48}$$

$$\mathbb{M}^{(2)}_{\mathbb{K}^{-1},i} \mathcal{N}^2_i (\boldsymbol{u}) = \left(\mathbb{E}^{3,2\intercal}_{i} \widetilde{\mathcal{N}}^0_i (p) - \mathbb{N}_{2i} \left(\widetilde{\mathcal{B}}^0 \left(\hat{p} \right)_i + \widetilde{\mathcal{B}}^0_i (\lambda) \right) \right) . \tag{49}$$

Note that (48) and (49) can be independently solved for each sub domain separately, and this step can be done in parallel. The interface variables λ serve as boundary conditions, compare with (40) and (41). Further details of computational implementation are given in Section 4.4.

4.4. Computational implementation

Algorithm 2: Algorithm for solving the DD formulation

construct global $\mathbb{E}^{3,2}$
construct global $\mathbb{N}_{2,i}$
for *all sub domains* **do**
  construct global $\mathbb{M}^{(2)}_{\mathbb{K}^{-1}}$
  evaluate Cholesky decomposition of $\mathbb{M}^{(2)}_{\mathbb{K}^{-1}}$ and save
  evaluate $\left(\mathbb{E}^{3,2} {\mathbb{M}^{(2)}_{\mathbb{K}^{-1}}}^{-1} \mathbb{E}^{3,2\intercal} \right)$ using Cholesky decomposition of $\mathbb{M}^{(2)}_{\mathbb{K}^{-1}}$
  evaluate Cholesky decomposition of $\left(\mathbb{E}^{3,2} {\mathbb{M}^{(2)}_{\mathbb{K}^{-1}}}^{-1} \mathbb{E}^{3,2\intercal} \right)$ and save
  evaluate LHS of (47)
  evaluate RHS of (47)
end
assemble LHS and RHS
evaluate Cholesky decomposition of LHS of (46)
solve (46) using MATLAB Cholesky solver
for *all sub domains* **do**
  evaluate $\widetilde{\mathcal{N}}^0_i (p)$ from (48) using Cholesky decomposition of $\left(\mathbb{E}^{3,2} {\mathbb{M}^{(2)}_{\mathbb{K}^{-1}}}^{-1} \mathbb{E}^{3,2\intercal} \right)$
  evaluate $\mathcal{N}^2_i (\boldsymbol{u})$ from (49) using Cholesky decomposition of $\mathbb{M}^{(2)}_{\mathbb{K}^{-1}}$
end

The system (45) is solved by static condensation, i.e. first for the global unknown $\widetilde{\mathcal{B}}^0 (\lambda)$, and then locally for the unknowns, $\widetilde{\mathcal{N}}^0_i (p)$ and $\mathcal{N}^2_i (\boldsymbol{u})$, in the sub domains.

First, we evaluate the mass matrix $\mathbb{M}^{(2)}_{\mathbb{K}^{-1},i}$, and then its Cholesky decomposition. Here, we use the MATLAB function `chol` [22] to evaluate the lower triangle matrix. Next we evaluate the matrix, $\left(\mathbb{E}^{3,2}_{i} {\mathbb{M}^{(2)}_{\mathbb{K}^{-1},i}}^{-1} \mathbb{E}^{3,2\intercal}_{i} \right)$ by using the lower triangular decomposition of $\mathbb{M}^{(2)}_{\mathbb{K}^{-1},i}$. Similar to the previous step, using MATLAB function `chol`, we evaluate the Cholesky decomposition of $\left(\mathbb{E}^{3,2}_{i} {\mathbb{M}^{(2)}_{\mathbb{K}^{-1},i}}^{-1} \mathbb{E}^{3,2\intercal}_{i} \right)$. Then, we can evaluate the left hand side and the right hand side of (47), for each sub domain separately. In the next step we assemble the left hand side and the right hand side systems of all the sub domains, to construct a global system of equations for the Lagrange multipliers λ.

The global system is solved by first evaluating the decomposition [21] and then using MATLAB solver to solve the system. Once the values of $\widetilde{\mathcal{B}}^0(\lambda)$ are obtained, the local unknowns are evaluated by Cholesky solver using decomposition of $\left(\mathbb{E}_i^{3,2}\mathbb{M}^{(2)}_{\mathbb{K}^{-1},i}{}^{-1}\mathbb{E}_i^{3,2\intercal}\right)$ and $\mathbb{M}^{(2)}_{\mathbb{K}^{-1},i}$, in a loop over all the sub domains, first for the unknown $\widetilde{\mathcal{N}}_i^0(p)$ and then for the unknown $\mathcal{N}_i^2(\boldsymbol{u})$.

4.5. Well-posedness

It remains to show that (45) is well-posed, i.e. its determinant is non-zero and the system of equations has a unique solution. To prove well-posedness, we must show that for the choice of right hand side terms $(\hat{p}, f, \hat{u}) = (\mathbf{0}_{\hat{p}}, \mathbf{0}_f, \mathbf{0}_{\hat{u}})$, the unique solution is given by $\mathcal{N}^2(\boldsymbol{u}), \widetilde{\mathcal{N}}^0(p), \widetilde{\mathcal{B}}^0(\lambda) = (\mathbf{0}_{\boldsymbol{u}}, \mathbf{0}_{\boldsymbol{p}}, \mathbf{0}_\lambda)$.

Before we start with the proof, we propose the following two Lemmas.

Lemma 1. *The incidence matrix $\mathbb{E}^{3,2}_{hyb}$ is surjective.*

Proof. Consider the divergence operator, $\mathbb{E}_i^{3,2}$, for any sub domain, $\mathcal{M}_i$. To prove that the discrete divergence operator $\mathbb{E}_i^{3,2}$ is surjective, we need to prove that for an arbitrary function $p \in \widetilde{S}(\mathcal{M}_i)$, there is a $\boldsymbol{q} \in D(\mathcal{M}_i)$ which is mapped by the divergence operator onto p. For this, we use an auxiliary problem: Find $\psi \in \widetilde{S}(\mathcal{M}_i)$ such that,

$$\operatorname{div} \widetilde{\operatorname{grad}}\,(\psi, 0) = p\ .$$

The variational formulation of this equation is given by

$$\int_{\mathcal{M}_i} \widetilde{\operatorname{grad}}\ (\phi, 0) \cdot \widetilde{\operatorname{grad}}\ (\psi, 0)\ \mathrm{d}\mathcal{M} = -\int_{\mathcal{M}_i} p\phi\ \mathrm{d}\mathcal{M}\ , \qquad \forall \phi \in \widetilde{S}(\mathcal{M}_i)\ .$$

Using the definition of weak grad, (20), and mass matrix of dual basis, the above equation is reduced to

$$\widetilde{\mathcal{N}}_i^0(\phi)^\intercal \mathbb{E}_i^{3,2}\left(\mathbb{M}_i^{(2)}\right)^{-1}\mathbb{E}_i^{3,2\intercal}\widetilde{\mathcal{N}}_i^0(\psi) = -\widetilde{\mathcal{N}}_i^0(\phi)^\intercal\left(\mathbb{M}_i^{(3)}\right)^{-1}\widetilde{\mathcal{N}}_i^0(p) \qquad \forall \phi \in \widetilde{S}(\mathcal{M}_i)\ ,$$

which has to hold for all vectors $\widetilde{\mathcal{N}}_i^0(\phi)$. Therefore we have

$$\mathbb{E}_i^{3,2}\left(\mathbb{M}_i^{(2)}\right)^{-1}\mathbb{E}_i^{3,2\intercal}\widetilde{\mathcal{N}}_i^0(\psi) = -\left(\mathbb{M}_i^{(3)}\right)^{-1}\widetilde{\mathcal{N}}_i^0(p)\ . \tag{50}$$

Using definition of weak gradient, where the operator $\mathbb{E}_i^{3,2\intercal}$ maps degrees of freedom from space $\widetilde{S}(\mathcal{M}_i)$ to the space $\widetilde{D}(\mathcal{M}_i)$, and Definition 1 where operator $\left(\mathbb{M}_i^{(2)}\right)^{-1}$ maps degrees of freedom from $\widetilde{D}(\mathcal{M}_i)$ to $D(\mathcal{M}_i)$ we define $\left(\mathbb{M}_i^{(2)}\right)^{-1}\mathbb{E}_i^{3,2\intercal}\widetilde{\mathcal{N}}_i^0(\psi) = -\mathcal{N}_i^2(\boldsymbol{u}) \in D(\mathcal{M}_i)$ in which case (50) can be written as

$$\mathbb{E}_i^{3,2}\mathcal{N}_i^2(\boldsymbol{u}) = \left(\mathbb{M}_i^{(3)}\right)^{-1}\widetilde{\mathcal{N}}_i^0(p)\ ,$$

or

$$\mathbb{M}_i^{(3)}\mathbb{E}_i^{3,2}\mathcal{N}_i^2(\boldsymbol{u}) = \widetilde{\mathcal{N}}_i^0(p)\ .$$

This equation states that for an arbitrary function $p \in \widetilde{S}(\mathcal{M}_i)$ there exists a vector $\boldsymbol{u} \in D(\mathcal{M}_i)$ which is mapped by the discrete divergence operator, $\mathbb{E}_i^{3,2}$ to degrees of freedom in $S(\mathcal{M}_i)$ and then mapped by the mass matrix $\mathbb{M}_i^{(3)}$ onto $\widetilde{S}(\mathcal{M}_i)$.

Since the divergence operator $\mathbb{E}^{3,2}_{hyb}$ is composed of block diagonal $\mathbb{E}_i^{3,2}$, it is also surjective by construction. □

Lemma 2. *Injectivity/Surjectivity of inclusion/trace map.*

Proof. Let $\iota : \Omega \to \partial\Omega$ be a continuous inclusion map. Then

$$\int_{\partial\Omega} \operatorname{tr} a^{(n-1)}\ \mathrm{d}\Gamma = \int_{\iota(\Omega)} \operatorname{tr} a^{(n-1)}\ \mathrm{d}\Gamma = \int_\Omega \iota^\star(\operatorname{tr} a^{(n-1)})\ \mathrm{d}\Omega\ .$$

Clearly, ι is surjective. The discrete analogue of this inclusion map is the inclusion matrix $\mathbb{N}$ and its trace is $\mathbb{N}^\intercal$. Also see Example 1, in Appendix. □

Now, let us start with the proof of well-posedness of (45). If the right hand side terms of (45) are zero, finite dimensional variational formulation (44) is given by

$$\begin{cases} \mathcal{N}^2(\boldsymbol{v})^\intercal \mathbb{M}^{(2)}_{\mathbb{K}^{-1},hyb} \mathcal{N}^2(\boldsymbol{u}) & -\mathcal{N}^2(\boldsymbol{v})^\intercal \mathbb{E}^{3,2\,\intercal}_{hyb} \widetilde{\mathcal{N}}^0(p) & +\mathcal{N}^2(\boldsymbol{v})^\intercal \mathbb{N}_2 \widetilde{\mathcal{B}}^0(\lambda) & = 0 & \forall\, \mathcal{N}^2(\boldsymbol{v}) \in D(\Omega_T) \\ -\widetilde{\mathcal{N}}^0(q)^\intercal \mathbb{E}^{3,2}_{hyb} \mathcal{N}^2(\boldsymbol{u}) & & & = 0 & \forall \widetilde{\mathcal{N}}^0(q) \in \widetilde{S}(\Omega_T) \\ \widetilde{\mathcal{B}}^0(\mu)^\intercal \mathbb{N}_2^\intercal \mathcal{N}^2(\boldsymbol{u}) & & & = 0 & \forall \widetilde{\mathcal{B}}^0(\mu) \in \widetilde{D}_b\left(\overset{\circ}{\Gamma} \cup \Gamma_N\right) \end{cases} . \tag{51}$$

The first equation is valid for all $\boldsymbol{v} \in D(\Omega)$, then it should also be valid for the solution $\boldsymbol{u} \in D(\Omega)$, which gives

$$\mathcal{N}^2(\boldsymbol{u})^\intercal \mathbb{M}^{(2)}_{\mathbb{K}^{-1},hyb} \mathcal{N}^2(\boldsymbol{u}) - \mathcal{N}^2(\boldsymbol{u})^\intercal \mathbb{E}^{3,2\,\intercal}_{hyb} \widetilde{\mathcal{N}}^0(p) + \mathcal{N}^2(\boldsymbol{u})^\intercal \mathbb{N}_2 \widetilde{\mathcal{B}}^0(\lambda) = 0 . \tag{52}$$

If we consider the second equation, as it is valid for all $q \in \widetilde{S}(\Omega)$, then it should also be valid for the solution $p \in \widetilde{S}(\Omega)$ of the equation, which gives

$$\widetilde{\mathcal{N}}^0(p)^\intercal \mathbb{E}^{3,2}_{hyb} \mathcal{N}^2(\boldsymbol{u}) = 0 .$$

If we take transpose on both the sides, we get

$$\mathcal{N}^2(\boldsymbol{u})^\intercal \mathbb{E}^{3,2\intercal}_{hyb} \widetilde{\mathcal{N}}^0(p) = 0 . \tag{53}$$

Similarly, the last equation is valid for all $\mu \in \widetilde{D}_b\left(\overset{\circ}{\Gamma} \cup \Gamma_N\right)$, then it should also be valid for the solution $\lambda \in \widetilde{D}_b\left(\overset{\circ}{\Gamma} \cup \Gamma_N\right)$, which gives

$$\mathcal{N}^2(\boldsymbol{u})^\intercal \mathbb{N}_2 \widetilde{\mathcal{B}}^0(\lambda) = 0 . \tag{54}$$

Substituting, (53) and (54) in (52), we get

$$\mathcal{N}^2(\boldsymbol{u})^\intercal \mathbb{M}^{(2)}_{\mathbb{K}^{-1},hyb} \mathcal{N}^2(\boldsymbol{u}) = 0 .$$

Since, $\mathbb{M}^{(2)}_{\mathbb{K}^{-1},hyb}$ is positive definite by construction, we have that $\mathcal{N}^2(\boldsymbol{u}) = \mathbf{0}$.

The first equation is now reduced to

$$\mathcal{N}^2(\boldsymbol{v})^\intercal \mathbb{E}^{3,2\,\intercal}_{hyb} \widetilde{\mathcal{N}}^0(p) + \mathcal{N}^2(\boldsymbol{v})^\intercal \mathbb{N}_2 \widetilde{\mathcal{B}}^0(\lambda) = 0 \qquad \forall\, \mathcal{N}^2(\boldsymbol{v}) \in D(\Omega) ,$$

and it remains to show that $\widetilde{\mathcal{N}}^0(p) = 0$, and $\widetilde{\mathcal{B}}^0(\lambda) = 0$.

Since, by Lemma 1, $\mathbb{E}^{3,2}_{hyb}$ is a surjective map from surface degrees of freedom to volumetric degrees of freedom, for any vector $\mathcal{N}^3(q)$ there exists a vector $\mathcal{N}^2(\boldsymbol{v})$, such that we can write

$$\mathcal{N}^3(q) = \mathbb{E}^{3,2}_{hyb} \mathcal{N}^2(\boldsymbol{v}) .$$

Therefore, we have that

$$\mathcal{N}^2(\boldsymbol{v})^\intercal \mathbb{E}^{3,2\,\intercal}_{hyb} \widetilde{\mathcal{N}}^0(p) = \mathcal{N}^3(q)^\intercal \widetilde{\mathcal{N}}^0(p) = 0 \Rightarrow \widetilde{\mathcal{N}}^0(p) = 0 \qquad \forall\, q \in S(\Omega_T) ,$$

which is another way of saying that if a matrix A is surjective, its transpose is injective.

Similarly, since by Lemma 2, $\mathbb{N}_2$ is a surjective map, any vector $\mathcal{B}^2(\mu)$ can be written as

$$\mathcal{B}^2(\mu) = \mathbb{N}_2 \mathcal{N}^2(\boldsymbol{v}) ,$$

and a similar argument reveals that the only solution is that $\widetilde{\mathcal{B}}^0(\lambda) = 0$.

This shows that the discrete Darcy problem using broken FE spaces defined in Section 3.3, is well-posed.

5. Test cases

In this section we present the computational results for two test cases using the DD formulation. All the simulations are executed on MATLAB release 2020b on a Macintosh machine with 2.6 GHz Intel Core i7 processor.

5.1. Test case I: Manufactured solution

In this section we will solve a test problem from [19] and compare the results of the DD formulation with the continuous formulation for elements of order $N = 1, 2, 3$ with varying mesh refinements. We will show that (i) the results from both formulations are the same up to machine precision, (ii) that the DD formulation has optimal convergence rates, (iii) the speed-up in simulation run times using the DD formulation, and (iv) comparison of condition number of (40) and (46).

The domain for the problem is obtained by mapping the reference domain $(\xi\ ,\eta\ ,\zeta) \in \widehat{\Omega} = [-1, 1]^3$ by

$$\begin{cases} x = \hat{x} + 0.03\cos\left(3\pi\hat{x}\right)\cos\left(3\pi\hat{y}\right)\cos\left(3\pi\hat{z}\right) \\ y = \hat{y} - 0.04\cos\left(3\pi\hat{x}\right)\cos\left(3\pi\hat{y}\right)\cos\left(3\pi\hat{z}\right) \\ z = \hat{z} + 0.05\cos\left(3\pi\hat{x}\right)\cos\left(3\pi\hat{y}\right)\cos\left(3\pi\hat{z}\right) \end{cases} \quad \text{where,} \quad \begin{cases} \hat{x} = 0.5\,(1+\xi) \\ \hat{y} = 0.5\,(1+\eta) \\ \hat{z} = 0.5\,(1+\zeta) \end{cases} . \tag{55}$$

In Fig. 2, in the left plot we show the reference domain $\widehat{\Omega}$ and on the right plot we show the domain of the problem which is obtained using (55).

The permeability tensor, $\mathbb{K}$, and the exact solution, p_{ex}, are given by

$$\mathbb{K}(x, y, z) = \begin{bmatrix} x^2+y^2+1 & 0 & 0 \\ 0 & z^2+1 & \sin(xy) \\ 0 & \sin(xy) & x^2y^2+1 \end{bmatrix}, \quad \text{and} \quad p_{ex}(x, y, x) = x + y + z - 1.5\ ,$$

and the right hand side term is given by

$$f_{ex} = -\text{div}\ \mathbb{K}\text{grad}\, p_{ex}\ .$$

As in [19], we impose the Dirichlet boundary conditions $\hat{p}$ at $\hat{x} = 0, 1$ faces and Neumann boundary conditions $\hat{u}$ at $\hat{y} = 0, 1, \hat{z} = 0, 1$ faces, where

$$\hat{p} = p_{ex}|_{\Gamma_D} \qquad \text{and} \qquad \hat{u} = (-\mathbb{K}\text{grad}\, p_{ex} \cdot \boldsymbol{n})\,|_{\Gamma_N}\ .$$

For the DD formulation of this test case we decompose the domain Ω in an equal number of sub domains, K_1, in each direction. For the $N = 1, 2$ cases each of the sub domains is further discretized into $2 \times 2 \times 2$ elements. For $N = 3$ case each sub domain consists of a single element only. Therefore, the total number of elements in one direction, K, are $K = 2K_1$ for $N = 1, 2$ case, and $K = K_1$ for $N = 3$ case. We define $\widehat{h} = 2/K$ as the size of an element of the reference domain $\widehat{\Omega} = [-1, 1]^3$.

5.1.1. Error convergence analysis

In Fig. 3 we present the pressure and velocity components of the DD formulation, and the difference between the continuous and the DD formulation for $K = 3, N = 2$ case. In the first row we plot the pressure, in the second row we plot the x-component of the velocity, in the third row we plot the y-component of the velocity, and in the fourth row we plot the z-component of the velocity. In the first column we plot the results from the DD formulation and in the second column we plot the difference of results between the continuous and the DD formulation. We see that the solution is the same up to machine precision for both the formulations and the maximum difference between the continuous and the DD formulation for any of the pressure or velocity field is of the order $\mathcal{O}\left(10^{-13}\right)$.

In Fig. 4 we show the convergence results for the DD formulation. At the top-left we show the convergence of the L^2-error for the constraint (div $\boldsymbol{u} - f_{ex}$), at the top right we show the convergence of the error for the velocity field in the H (div; Ω) norm, and in the bottom-centre we show the convergence of the error for the pressure field in the weak $H^1(\Omega)$ norm (using (36)). On the x-axis we have the length of the non-deformed element $\widehat{h}$. The error and convergence rates of the continuous formulation and the DD formulation are same up to machine precision. All the error plots show optimal rate of convergence of order $\mathcal{O}(N)$.

5.1.2. Simulation times

In Table 1, Table 2, Table 3 we give the average simulation times to solve the continuous formulation, the DD formulation, and the comparison between the two cases respectively. The simulation time (in seconds) is the average for five simulation runs.

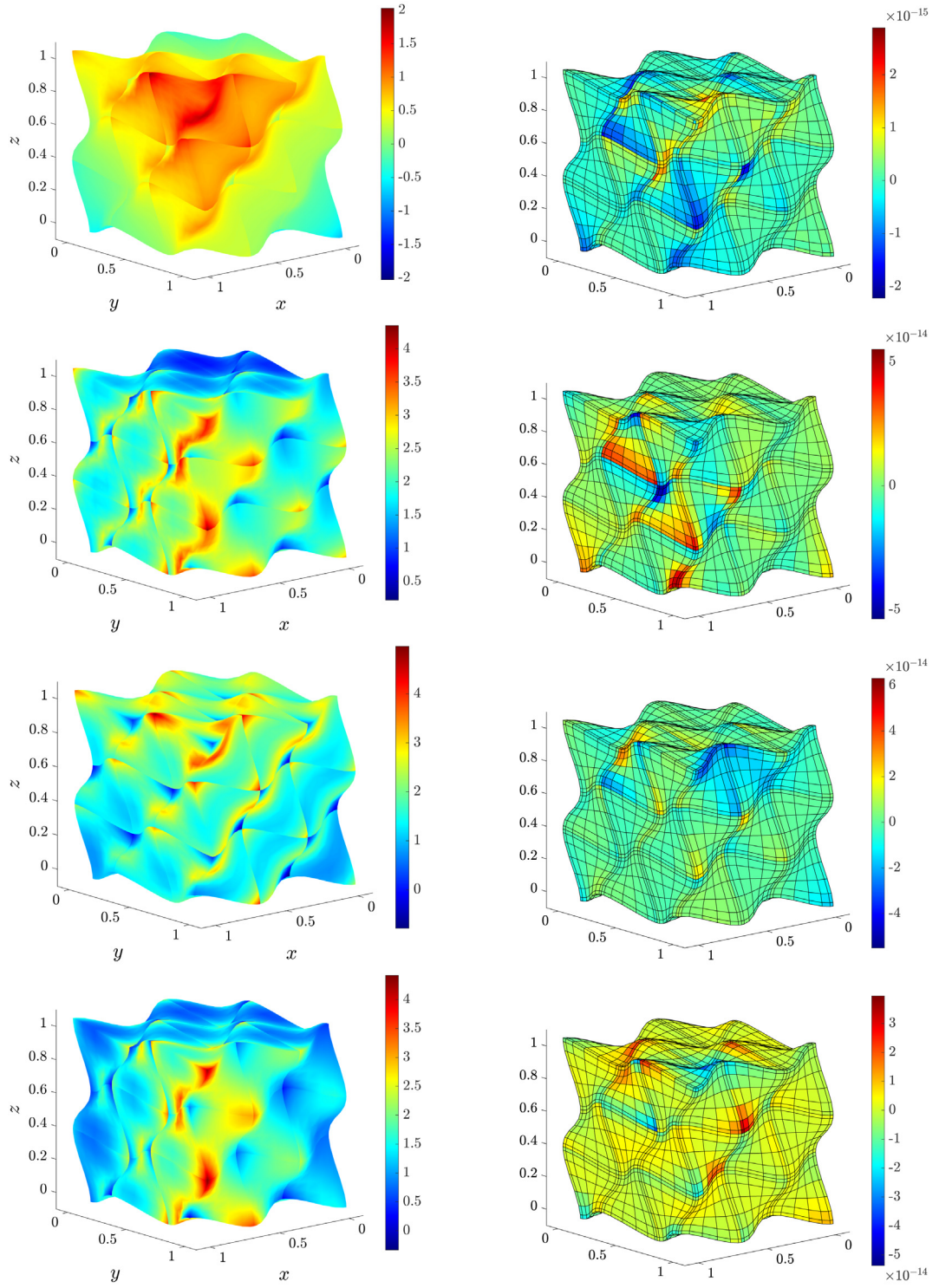

Fig. 3. Comparison of pressure and velocity profiles for the continuous formulation and the DD formulation for $K = 3, N = 2$ case. In the first column we see the results of the DD formulation, and in the second column we present the difference between the results of the continuous and the DD formulation. In the first row we see the pressure, in the second row the x-component of the velocity field, in the third row the y-component of the velocity field and in the fourth row the z-component of the velocity field.

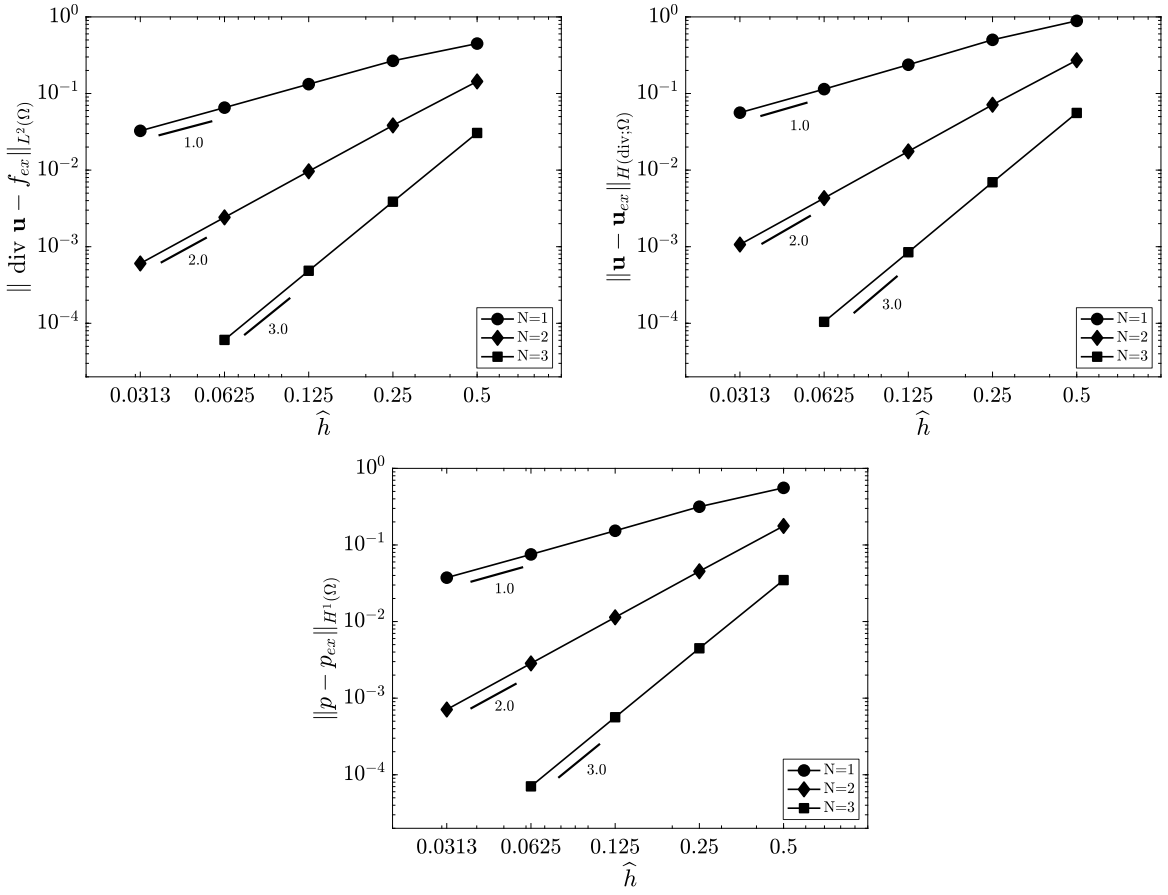

Fig. 4. Convergence results for the DD formulation. Top left: Error $(\text{div}\,\boldsymbol{u} - f_{ex})$ in $L^2(\Omega)$ norm. Top right: Error $(\boldsymbol{u} - \boldsymbol{u}_{ex})$ in $H(\text{div};\Omega)$ norm. Bottom centre: Error $(p - p_{ex})$ in the weak $H^1(\Omega)$ norm.

In Table 1, we give the average simulation time to solve for continuous formulation for elements of order $N = 1, 2, 3$. In the first column we have the number of elements in one direction, in the second column we have the time taken to set-up the matrices (this also includes the time taken for Cholesky decomposition of $\mathbb{M}^{(2)}_{\mathbb{K}^{-1}}$), in the third column the time taken to solve (40) and (41) and in the fourth column the total simulation time. The simulation times that are less than 0.1 s, have not been measured with further accuracy.

In Table 2, we give the average simulation time to solve for DD formulation for elements of order $N = 1, 2, 3$. In the first column, we give the total number of elements in one direction, K. In the second column we give the number of sub domains in one direction, K_1. In the third column we give the number of elements in each direction within each sub domain, K_2. In the fourth column we give the time to set-up the matrices (this includes the time to calculate the Cholesky decomposition of $\mathbb{M}^{(2)}_{\mathbb{K}^{-1},i}$ and $\left(\mathbb{E}^{3,2}_i \mathbb{M}^{(2)}{}^{-1}_{\mathbb{K}^{-1},i} \mathbb{E}^{3,2\intercal}_i\right)$ for all the sub domains). In the fifth column we give the time to solve the global system of Lagrange multiplier (46), i.e. decomposition of the left hand side of (46) and the solution. In the sixth column we give the time to solve for the pressure unknowns (48) and the velocity unknowns (49) over all the sub domains. In the seventh column we give the total time, and in the eighth column we give the % amount of time spent to evaluate (46). For the cases where simulation times are less than 0.1 s the accurate simulation times are not determined and therefore we do not calculate the last column. We observe in the last column that for all the three cases i.e. $N = 1, 2, 3$, as we increase the total number of sub domains the percentage of time spent on solution of the Lagrange multiplier system increases. In the most refined mesh case for $N = 1, 2, 3$, the time spent in solution of (46) is above 80%. Given that the objective of DD formulation is to solve large simulations, we see that majority of the time is spent on solution of the Lagrange multiplier system

Table 1
Average computational time (in seconds) for set-up and solution of the continuous elements formulation.

	K	Set-up time	Solve time	Total time
$N = 1$				
	4	< 0.1	< 0.1	< 0.2
	8	< 0.1	< 0.1	< 0.2
	16	0.2	7.1	7.3
	20	0.4	34.3	34.7
	24	0.8	118.7	119.5
	28	1.5	369.6	371.1
	32	2.6	1276.5	1279.1
$N = 2$				
	4	< 0.1	< 0.1	< 0.2
	8	< 0.1	< 0.1	< 0.2
	12	0.4	92.7	93.1
	16	1.3	1058.1	1059.4
$N = 3$				
	4	< 0.1	< 0.1	< 0.2
	6	0.2	14.0	14.2
	8	0.5	95.6	96.1

Table 2
Average computational time (in seconds) for set-up and solution of the DD formulation.

	K	K_1	K_2	Set-up time	Solve (46)	Solve (48) & (49)	Total	% to solve (46)
$N = 1$								
	4	2	2	< 0.1	< 0.1	< 0.1	< 0.3	–
	8	4	2	< 0.1	< 0.1	< 0.1	< 0.3	–
	16	8	2	0.5	< 0.1	< 0.1	< 0.7	–
	20	10	2	1.0	< 0.1	< 0.1	< 1.2	–
	24	12	2	1.7	< 0.1	< 0.1	< 1.9	–
	28	14	2	2.7	0.2	< 0.1	< 3.0	–
	32	16	2	4.0	0.4	< 0.1	< 4.5	–
	64	32	2	32.1	22.3	1.0	55.4	40.25%
	128	64	2	263.0	2180.1	20.0	2463.1	88.51%
$N = 2$								
	4	2	2	< 0.1	< 0.1	< 0.1	< 0.3	–
	8	4	2	0.2	< 0.1	< 0.1	< 0.4	–
	12	6	2	0.7	< 0.1	< 0.1	< 1.0	–
	16	8	2	1.7	0.3	0.2	< 2.2	–
	32	16	2	16.4	12.9	1.8	31.1	41.48%
	64	32	2	268.9	1959.6	56.3	2284.8	85.77%
$N = 3$								
	4	4	1	< 0.1	< 0.1	< 0.1	< 0.3	–
	6	6	1	0.5	< 0.1	< 0.1	< 0.7	–
	8	8	1	0.8	< 0.1	< 0.1	< 1.0	–
	16	16	1	6.0	3.0	0.4	9.4	31.91%
	32	32	1	49.6	290.8	11.8	352.2	82.57%

(46). This also directs attention to the second challenge for DD methods mentioned in the introduction, that is to find an efficient way to solve the global Lagrange multiplier system.

In Table 3 we compare the total time taken to solve the continuous formulation and the DD formulation for elements of order $N = 1, 2, 3$. The comparison is made for cases where the topology of the mesh discretization

Table 3
Average computational time (in seconds) for the (i) continuous formulation, (ii) DD formulation, and the speed-up in simulation time (56).

	K	Continuous	DD	Speed-up
$N = 1$				
	16	7.3	< 0.7	10.4
	20	34.7	< 1.2	28.9
	24	119.5	< 1.9	62.9
	28	371.1	< 3.0	123.7
	32	1279.1	< 4.5	284.2
$N = 2$				
	12	93.1	< 1.0	93.1
	16	1059.4	< 2.2	481.5
$N = 3$				
	6	14.2	< 0.7	20.3
	8	96.1	< 1.0	96.1

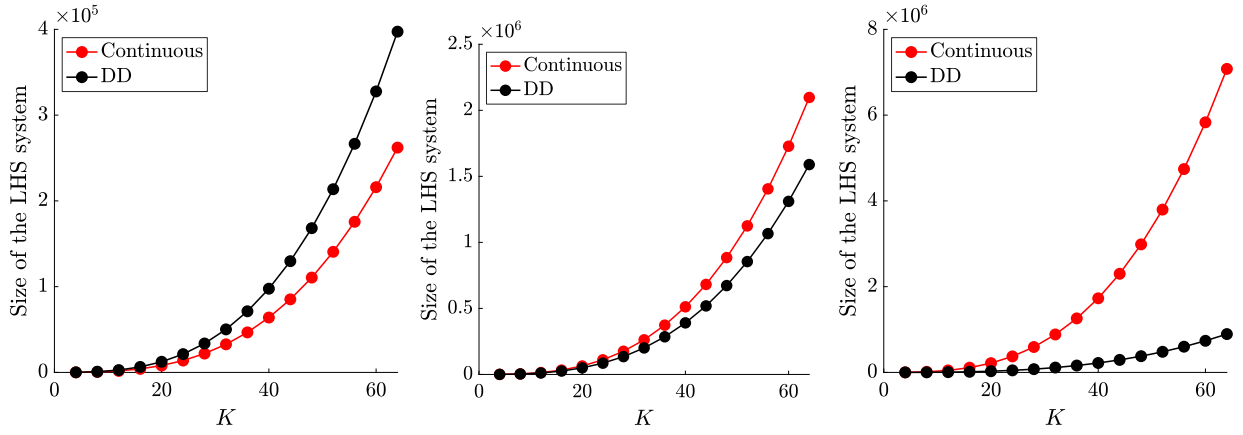

(a) N=1 (b) N=2 (c) N=3

Fig. 5. Comparison of the size of the left hand side system for cases $N = 1, 2, 3$ for continuous formulation (40), and DD formulation (46).

remains the same. In the first column we have the total number of elements in one direction K, in the second column we have the total simulation time from continuous formulation, in the third column we have the total simulation time from DD formulation. In the fourth column we give the speed-up factor as

$$\text{speed-up} = \frac{\text{simulation time continuous formulation}}{\text{simulation time DD formulation}} . \tag{56}$$

Firstly, the simulation time required for the same refinement is less for the DD formulation than for the continuous formulation in all the cases. Secondly, the speed-up factor increases as the mesh is more refined. Therefore, a DD formulation is more advantageous in case of large simulations.

5.1.3. Size of the system matrices

In Table 1 we have seen that for the continuous formulation the maximum time is spent on solving the pressure unknown (40), and in Table 2 we have seen that the maximum time is spent to solve the Lagrange multiplier Eq. (46). In Fig. 5 we compare the size of the left hand side systems for these equations for the same number of total elements and topological discretization, for cases $N = 1, 2, 3$. On the x-axis we have K, the total number of elements in one direction, and on the y-axis we have the size of the left hand size system.

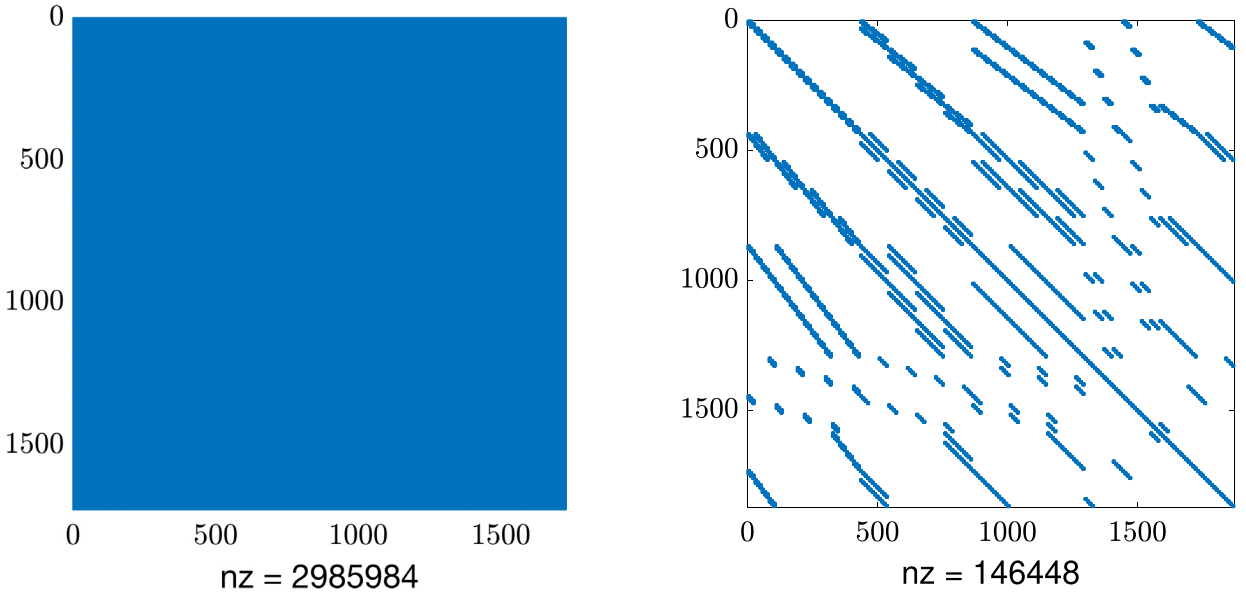

Fig. 6. Sparsity plot of the left hand side system of (i) Left plot: (40) for $K = 4, N = 3$, (ii) Right plot: (46) for $K1 = 4, K2 = 1, N = 3$.

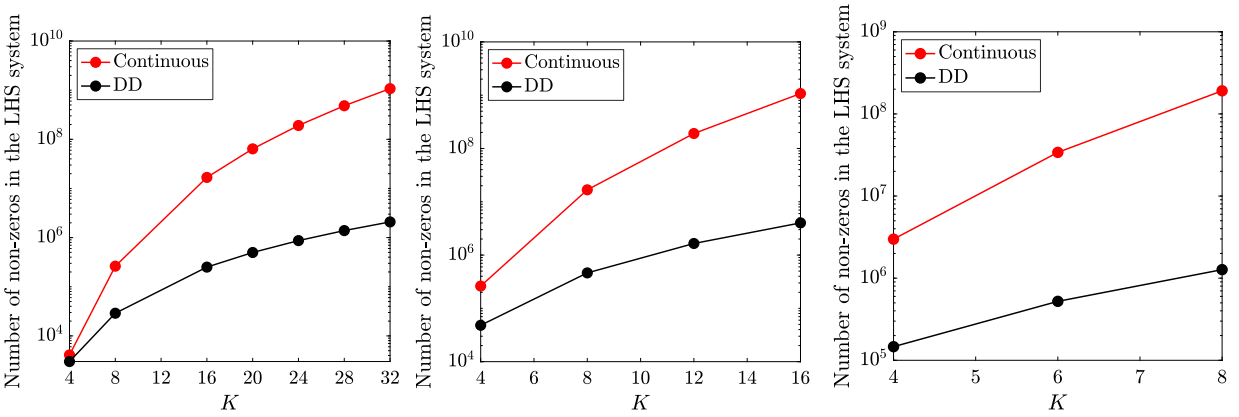

Fig. 7. Comparison of the number of non zeros in the left hand side system for cases $N = 1, 2, 3$ for the continuous formulation (40), and the DD formulation (46).

For the $N = 1$ case the size of the λ system of the DD formulation is bigger than the size of the pressure unknown system of the continuous formulation. Even then, the simulation time to solve the λ system is less. For $N = 2$ and $N = 3$ case we see that the size of the left hand side system grows less for the DD formulation than for the continuous formulation, upon mesh refinement.

In Fig. 6 we show the sparsity plot for the left hand system of (40) and (46) for similar topological configuration of total number of elements = $4 \times 4 \times 4$ and $N = 3$. We see in the left plot that system for the continuous formulation is a full matrix with number of non-zeros = 2985984, whereas the left hand side of the Lagrange multiplier system is sparse with number of non-zeros = 146448.

In Fig. 7, we compare the number of non zeros in the left hand side system of (40) and (46), for the cases $N = 1, 2, 3$. We see that the number of non-zeros in continuous case grow more rapidly than in the DD case, in all the three cases.

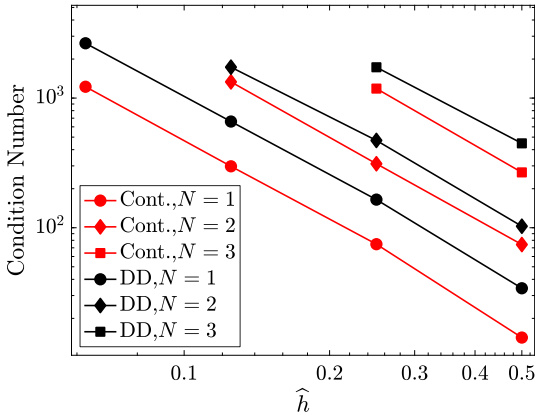

Fig. 8. Comparison of condition number of (40) and (46) for $N = 1, 2, 3$.

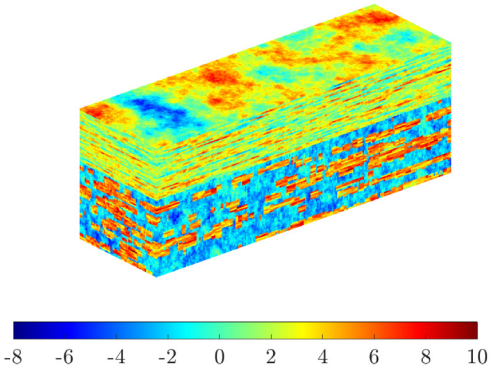

Fig. 9. Natural logarithm of permeability field for SPE10 case.

In Fig. 8 we compare the condition number of the global system of (40) and (46) for $N = 1, 2, 3$. In all the cases, we observe similar rate of growth of condition number for the continuous formulation and the DD formulation. Furthermore, for the same discretization, the condition number of the Lagrange multiplier system (46) is higher than the condition number of the pressure unknowns of (40), even though the Lagrange multiplier system has much less degrees of freedom, and number of non-zeros in the left hand side system. This further emphasizes, the need to use an appropriate preconditioner, for eg. the ones developed in [23,24], when solving the Lagrange multiplier system with iterative methods.

5.2. Test case II: SPE 10

In this section we show the results for the SPE10 benchmark problem [20]. It is often used for validation of numerical schemes for reservoir modelling applications because of its challenging permeability field. The domain of the problem and the natural logarithm of the permeability field is shown in Fig. 9. The size of the domain is 1200 ft $\times$ 2200 ft $\times$ 170 ft. The domain is divided into equal blocks of size 20 ft $\times$ 10 ft $\times$ 2 ft, i.e. $60 \times 220 \times 85 = 1122000$ blocks. Each block has a constant isotropic permeability tensor $\mathbb{K}_i = k_i \mathbb{I}$. The top 70 ft of the domain represents the Tarbert formation that has smooth changes in the permeability field component, and the bottom 100 ft represents the Upper Ness formation that has sharp changes in the permeability field component.

The right hand side term is $f_{ex} = 0$. We impose Neumann boundary conditions, $\hat{u} = \boldsymbol{u} \cdot \boldsymbol{n} = 0$, on $\hat{y}, \hat{z} = 0, 1$ faces, and the Dirichlet boundary conditions, $\hat{p} = 1$ on $\hat{x} = 0$ face, and $\hat{p} = 0$ on $\hat{x} = 1$ face.

For the numerical solution using the DD method, we use two different approaches. In *Case* 1, we divide the domain into 15 $\times$ 55 $\times$ 17 sub domains, and each sub domain is further divided into 4 $\times$ 4 $\times$ 5 elements. In *Case* 2,

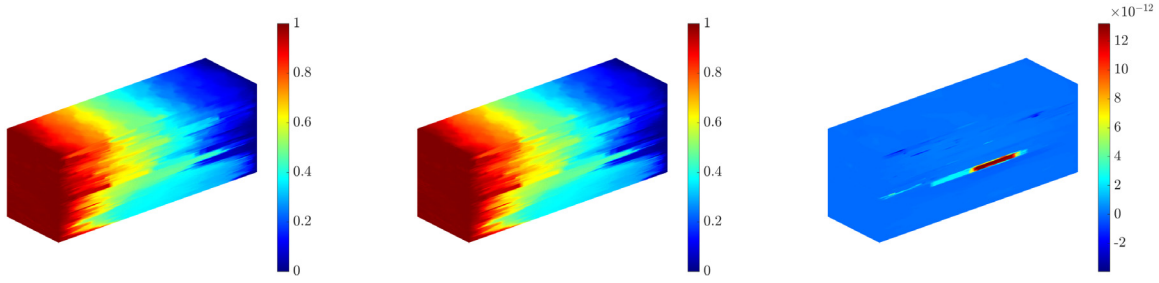

Fig. 10. The contour plots of pressure field for SPE10 benchmark problem. Left: results from *Case* 1. Centre: results from *Case* 2. Right: difference between results from *Case* 1 and *Case* 2.

Table 4
Average computational time (in seconds) for set-up and solution of SPE10 case using DD formulation.

	$K_x \times K_y \times K_z$	$K_{1x} \times K_{1y} \times K_{1z}$	$K_{2x} \times K_{2y} \times K_{2z}$	Set-up time	Solve (46)	Solve (48) & (49)	Total	% (46)
Case 1	1122000	$15 \times 55 \times 17$	$4 \times 4 \times 5$	154.0	259.4	20.4	433.8	59.8%
Case 2	1122000	$12 \times 44 \times 17$	$5 \times 5 \times 5$	184.2	159.5	24.3	368.0	43.3%

we divide the domain into $12 \times 44 \times 17$ sub domains, and each sub domain is further divided into $5 \times 5 \times 5$ elements. The total number and topological configuration of the elements remain the same in all the cases. We use only the lowest order elements, i.e. $N = 1$, in both the cases. The results of the pressure field from both the cases are shown in Fig. 10. In the left plot we see the results from *Case* 1, in the centre plot we see the results from *Case* 2, and in the right plot we see the difference between the two results. We observe that the solution is exact up to machine precision in both the cases, independent of the decomposition of the domain, with maximum difference in results of the order of $\mathcal{O}\left(10^{-12}\right)$.

In Table 4 we give the average run time of five simulation runs to solve the SPE10 case (in seconds) using the DD formulation. In the second column we have the total number of elements, in the third column we have the total number of sub domains, in the fourth column we have the total number of elements within each sub domain, in the fifth column we have the set-up time of matrices (including the time take to inverse the matrices $\mathbb{M}^{(2)}_{\mathbb{K}^{-1},i}$ and $\left(\mathbb{E}^{3,2}_i \mathbb{M}^{(2)}{}^{-1}_{\mathbb{K}^{-1},i} \mathbb{E}^{3,2}_i\right)$), in the sixth column we have the time taken to solve the Lagrange multiplier system (46), in the seventh column we have the time taken to solve the pressure unknowns (48) and the velocity unknowns (49), in the eighth column we have the total time, and in the ninth column we have the % of time taken to solve the Lagrange multiplier system (46) with respect to the total time. The results show that for the same total number and topology of elements, the choice of sub domain decomposition affects the simulation times.

This test case demonstrates that use of algebraic dual spaces with a DD method can be applied to practical applications.

6. Conclusions

In this paper we have presented the use of algebraic dual spaces for DD formulation of Darcy flow. We have defined the broken Sobolev spaces and their finite dimensional counterparts. We have also defined the global finite dimensional trace space that connects the broken spaces. These spaces are then used to solve the DD formulation of Darcy equations. It is shown that using algebraic dual spaces the matrix representation of the constraint on divergence of velocity, the pressure gradient term and the continuity constraint across the sub domains becomes sparse and metric-free. The first test case is a manufactured solution where it is shown that (i) the results from the continuous formulation and the DD formulation are exact up to machine precision and that DD formulation has optimal rate of convergence of errors, (ii) the DD formulation is more efficient in terms of simulation run times. In the second test case we show that DD scheme can be used to solve for practical applications.

There are two immediate steps for future work. The first is to improving the efficiency of solving the global Lagrange multiplier system. For example, by investigating a hierarchical DD method or using an iterative solver with a suitable preconditioner for solving (46). The second, in this work we have used broken $H\,(\mathrm{div};\,\Omega)$ and

$L^2(\Omega)$ spaces. In future this work will be extended to broken $H^1(\Omega)$ and $H(\text{curl};\Omega)$ spaces, to address problems such as vector Laplacian, Stokes flow, and linear elasticity.

Declaration of competing interest

The authors declare the following financial interests/personal relationships which may be considered as potential competing interests: Varun Jain reports financial support was provided by Nederlandse Organisate voor Wetenschappelijk Onderzoek Utrecht.

Data availability

Data will be made available on request.

Acknowledgements

Varun Jain is supported by the Shell-NWO PhD75, The Netherlands Grant P/fom-d-69/3. The authors would like to thank Dr. Hadi Hajibeygi for the processed permeability data of the SPE10 benchmark case.

Appendix. Examples of the inclusion matrix and the divergence operator

Example 1. In Fig. 2, on the left plot we show a domain $[-1,1]^3 \subset \mathbb{R}^3$ discretized into $2 \times 2 \times 2$ volumes. The inclusion map $\mathbb{N}_2$ for this domain is given by

$$\mathbb{N}_2^{\intercal} = \begin{bmatrix}
0&0&0&0&0&0&0&0&0&0&0&0&1&0&0&0&0&0&0&0&0&0&0&0&0&0&0&0&0&0&0&0&0&0&0&0\\
0&0&0&0&0&0&0&0&0&0&0&0&0&1&0&0&0&0&0&0&0&0&0&0&0&0&0&0&0&0&0&0&0&0&0&0\\
0&0&0&0&0&0&0&0&0&0&0&0&0&0&1&0&0&0&0&0&0&0&0&0&0&0&0&0&0&0&0&0&0&0&0&0\\
0&0&0&0&0&0&0&0&0&0&0&0&0&0&0&1&0&0&0&0&0&0&0&0&0&0&0&0&0&0&0&0&0&0&0&0\\
0&0&0&0&0&0&0&0&0&0&0&0&0&0&0&0&0&0&1&0&0&0&0&0&0&0&0&0&0&0&0&0&0&0&0&0\\
0&0&0&0&0&0&0&0&0&0&0&0&0&0&0&0&0&0&0&1&0&0&0&0&0&0&0&0&0&0&0&0&0&0&0&0\\
0&0&0&0&0&0&0&0&0&0&0&0&0&0&0&0&0&0&0&0&1&0&0&0&0&0&0&0&0&0&0&0&0&0&0&0\\
0&0&0&0&0&0&0&0&0&0&0&0&0&0&0&0&0&0&0&0&0&1&0&0&0&0&0&0&0&0&0&0&0&0&0&0\\
0&0&0&0&0&0&0&0&0&0&0&0&0&0&0&0&0&0&0&0&0&0&1&0&0&0&0&0&0&0&0&0&0&0&0&0\\
0&0&0&0&0&0&0&0&0&0&0&0&0&0&0&0&0&0&0&0&0&0&0&1&0&0&0&0&0&0&0&0&0&0&0&0\\
0&0&0&0&0&0&0&0&0&0&0&0&0&0&0&0&0&0&0&0&0&0&0&0&1&0&0&0&0&0&0&0&0&0&0&0\\
0&0&0&0&0&0&0&0&0&0&0&0&0&0&0&0&0&0&0&0&0&0&0&0&0&1&0&0&0&0&0&0&0&0&0&0\\
0&0&0&0&0&0&0&0&0&0&0&0&0&0&0&0&0&0&0&0&0&0&0&0&0&0&1&0&0&0&0&0&0&0&0&0\\
0&0&0&0&0&0&0&0&0&0&0&0&0&0&0&0&0&0&0&0&0&0&0&0&0&0&0&1&0&0&0&0&0&0&0&0\\
0&0&0&0&0&0&0&0&0&0&0&0&0&0&0&0&0&0&0&0&0&0&0&0&0&0&0&0&1&0&0&0&0&0&0&0\\
0&0&0&0&0&0&0&0&0&0&0&0&0&0&0&0&0&0&0&0&0&0&0&0&0&0&0&0&0&1&0&0&0&0&0&0\\
0&0&0&0&0&0&0&0&0&0&0&0&0&0&0&0&0&0&0&0&0&0&0&0&0&0&0&0&0&0&1&0&0&0&0&0\\
0&0&0&0&0&0&0&0&0&0&0&0&0&0&0&0&0&0&0&0&0&0&0&0&0&0&0&0&0&0&0&1&0&0&0&0\\
0&0&0&0&0&0&0&0&0&0&0&0&0&0&0&0&0&0&0&0&0&0&0&0&0&0&0&0&0&0&0&0&1&0&0&0\\
0&0&0&0&0&0&0&0&0&0&0&0&0&0&0&0&0&0&0&0&0&0&0&0&0&0&0&0&0&0&0&0&0&1&0&0\\
0&0&0&0&0&0&0&0&0&0&0&0&0&0&0&0&0&0&0&0&0&0&0&0&0&0&0&0&0&0&0&0&0&0&1&0\\
0&0&0&0&0&0&0&0&0&0&0&0&0&0&0&0&0&0&0&0&0&0&0&0&0&0&0&0&0&0&0&0&0&0&0&1
\end{bmatrix}.$$

The domain has a total number of 36 faces, and 24 boundary faces. Therefore the dimension of $\mathbb{N}_2$ is 36×24. The outward unit normal at the $x = 1$ or $y = 1$ or $z = 1$ faces acts in the positive direction, and therefore we use $+1$ entry, and at the $x = -1$ or $y = -1$ or $z = -1$ faces it acts in the opposite direction and we use -1 entry. In the right plot of Fig. 2 we have a deformed domain, but the inclusion map remains the same.

The inclusion matrix is a sparse metric-free matrix, that consists of $+1$, -1 and 0 entries only, and is independent of shape and size of elements as long as the topology, numbering of the degrees of freedom and the orientation of the mesh remains the same.

Example 2. Divergence operator for 3D mesh

Let us consider Fig. 2 again. The expansion coefficients of $\mathcal{N}^2(\boldsymbol{u})$, are defined at the surfaces in the mesh. The divergence operation on any volume V_i, is then defined as

$$\int_{V_i} \operatorname{div} \boldsymbol{u} \, \mathrm{d}K = \int_{\partial V_i} \boldsymbol{u} \cdot \boldsymbol{n} \, \mathrm{d}\gamma = -\mathcal{N}^2(\boldsymbol{u})_{left} + \mathcal{N}^2(\boldsymbol{u})_{right} - \mathcal{N}^2(\boldsymbol{u})_{bottom} + \mathcal{N}^2(\boldsymbol{u})_{top} - \mathcal{N}^2(\boldsymbol{u})_{back} + \mathcal{N}^2(\boldsymbol{u})_{front} . \tag{57}$$

If we assemble (57) for all the 8 volumes, with appropriate numbering, we get the discrete divergence operator as

$$\mathbb{E}^{3,2} = \begin{bmatrix}
-1 & 1 & 0 & 0 & 0 & 0 & 0 & 0 & 0 & 0 & -1 & 0 & 1 & 0 & 0 & 0 & 0 & 0 & 0 & 0 & -1 & 0 & 0 & 0 & 1 & 0 & 0 & 0 & 0 & 0 \\
0 & -1 & 1 & 0 & 0 & 0 & 0 & 0 & 0 & 0 & 0 & -1 & 0 & 1 & 0 & 0 & 0 & 0 & 0 & 0 & 0 & 0 & -1 & 0 & 0 & 0 & 1 & 0 & 0 & 0 & 0 \\
0 & 0 & 0 & -1 & 1 & 0 & 0 & 0 & 0 & 0 & 0 & 0 & -1 & 0 & 1 & 0 & 0 & 0 & 0 & 0 & 0 & 0 & 0 & -1 & 0 & 0 & 0 & 1 & 0 & 0 & 0 & 0 \\
0 & 0 & 0 & 0 & -1 & 1 & 0 & 0 & 0 & 0 & 0 & 0 & 0 & -1 & 0 & 1 & 0 & 0 & 0 & 0 & 0 & 0 & 0 & 0 & -1 & 0 & 0 & 0 & 1 & 0 & 0 & 0 \\
0 & 0 & 0 & 0 & 0 & -1 & 1 & 0 & 0 & 0 & 0 & 0 & 0 & 0 & -1 & 0 & 1 & 0 & 0 & 0 & 0 & 0 & 0 & 0 & 0 & -1 & 0 & 0 & 0 & 1 & 0 & 0 \\
0 & 0 & 0 & 0 & 0 & 0 & -1 & 1 & 0 & 0 & 0 & 0 & 0 & 0 & 0 & -1 & 0 & 1 & 0 & 0 & 0 & 0 & 0 & 0 & 0 & 0 & -1 & 0 & 0 & 1 & 0 & 0 \\
0 & 0 & 0 & 0 & 0 & 0 & 0 & -1 & 1 & 0 & 0 & 0 & 0 & 0 & 0 & 0 & -1 & 0 & 1 & 0 & 0 & 0 & 0 & 0 & 0 & 0 & 0 & -1 & 0 & 0 & 1 & 0 \\
0 & 0 & 0 & 0 & 0 & 0 & 0 & 0 & -1 & 1 & 0 & 0 & 0 & 0 & 0 & 0 & 0 & -1 & 0 & 1 & 0 & 0 & 0 & 0 & 0 & 0 & 0 & 0 & -1 & 0 & 0 & 1
\end{bmatrix}.$$

We have 8 volumes and 36 faces, therefore dimension of $\mathbb{E}^{3,2}$ is 8×36. It is a sparse, metric free matrix that consists of $+1, -1, 0$ entries only. If the domain is deformed, for example see the right plot of Fig. 2, but the connection between the nodes, edges, surfaces, and volumes, remains the same, relation (57) remains the same and consequently the matrix $\mathbb{E}^{3,2}$ remains unchanged.

References

[1] T.H.H. Pian, P. Tong, Basis of finite element methods for solid continua, Internat. J. Numer. Methods Engrg. 1 (1969) 3–28, http://dx.doi.org/10.1002/nme.1620010103.

[2] P. Tong, T.H.H. Pian, S.J. Lasry, A hybrid-element approach to crack problems in plane elasticity, Internat. J. Numer. Methods Engrg. 7 (1973) 297–308, http://dx.doi.org/10.1002/nme.1620070307.

[3] P.A. Raviart, J.M. Thomas, Primal hybrid finite element methods for 2nd order elliptic equations, Math. Comp. 31 (1977) 391–413.

[4] V. Agoshkov, Poincaré–Steklov's operators and domain decomposition methods in finite-dimensional spaces, in: First International Symposium on Domain Decomposition Methods for Partial Differential Equations, SIAM, 1988, pp. 73–112.

[5] A. Quarteroni, A. Valli, Theory and application of Steklov-Poincaré operators for boundary-value problems, in: Mathematics and its Applications, Vol. 56, Springer, 1991, pp. 179–203.

[6] C. Farhat, J. Mandel, F.X. Roux, Optimal convergence properties of the FETI domain decomposition method, Comput. Methods Appl. Mech. Engrg. 115 (1994) 365–385.

[7] C. Farhat, M. Lesoinne, P. LeTallec, K. Pierson, D. Rixen, FETI-DP: a dual–primal unified FETI method—part I: A faster alternative to the two-level FETI method, Internat. J. Numer. Methods Engrg. 50 (7) (2001) 1523–1544.

[8] B. Wohlmuth, A mortar finite element method using dual spaces for the Lagrange multiplier, SIAM J. Numer. Anal. (2000) 989–1012.

[9] T.H. Pian, C.-C. Wu, Hybrid and Incompatible Finite Element Methods, CRC Press, 2005.

[10] C. Lacour, Y. Maday, Two different approaches for matching nonconforming grids: The Mortar element method and the FETI method, BIT Numer. Math. 37 (1997) 720–738, http://dx.doi.org/10.1007/BF02510249.

[11] C. Bernardi, Y. Maday, F. Rapetti, Basics and some applications of the mortar element method, GAMM-Mitt. 28 (2005) 97–123, http://dx.doi.org/10.1002/gamm.201490020.

[12] B. Cockburn, Static Condensation, Hybridization, and the Devising of the HDG Methods, in: Lecture Notes in Computational Science and Engineering, vol. 114, Springer, 2015, pp. 129–177.

[13] D. Pietro, A. Ern, S. Lemaire, A Review of Hybrid High Order Methods: Formulations, Computational Aspects, Comparison with Other Methods, in: Lecture Notes in Computational Science and Engineering, vol. 114, Springer, 2016, pp. 205–236.

[14] J.P.M. Almeida, E.A. Maunder, Equilibrium Finite Element Formulations, John Wiley & Sons Ltd, 2016.

[15] V. Jain, Y. Zhang, A. Palha, M. Gerritsma, Construction and application of algebraic dual polynomial representations for finite element methods on quadrilateral and hexahedral meshes, Comput. Math. Appl. 95 (2021) 101–142.

[16] M. Gerritsma, Edge functions for spectral element methods, in: Spectral and High Order Methods for Partial Differential Equations, Springer, 2011, pp. 199–208.

[17] J. Kreeft, M. Gerritsma, Mixed mimetic spectral element method for Stokes flow: A pointwise divergence-free solution, J. Comput. Phys. 240 (2013) 284–309.

[18] A. Palha, P.P. Rebelo, R. Hiemstra, J. Kreeft, M. Gerritsma, Physics-compatible discretization techniques on single and dual grids, with application to the Poisson equation of volume forms, J. Comput. Phys. 257 (2014) 1394–1422.

[19] M.F. Wheeler, G. Xue, I. Yotov, A multiscale mortar multipoint flux mixed finite element method, ESAIM Math. Model. Numer. Anal. 46 (2012) 759–796.

[20] SPE comparative solution project, URL https://www.spe.org/web/csp/datasets/set02.htm.

[21] Matrix decomposition for solving linear systems - MATLAB, URL https://www.mathworks.com/help/matlab/ref/decomposition.html.

[22] Cholesky factorization - MATLAB chol, URL https://www.mathworks.com/help/matlab/ref/chol.html.

[23] S. Zampini, X. Tu, Multilevel balancing domain decomposition by constraints deluxe algorithms with adaptive coarse spaces for flow in porous media, SIAM J. Sci. Comput. 39 (2017) 1389–1415, http://dx.doi.org/10.1137/16M1080653.

[24] F. Dassi, S. Zampini, S. Scacchi, Robust and scalable adaptive BDDC preconditioners for virtual element discretizations of elliptic partial differential equations in mixed form, Comput. Methods Appl. Mech. Engrg. 391 (2022) 114620, http://dx.doi.org/10.1016/j.cma.2022.114620.